Rapport nr. 86.042

On numerical AMT profiles and sounding curves over some two-dimensional structures

Norges geologiske undersøkelse

Leiv Eirikssons vei 39, Postboks 3006, 7001 Trondheim - Tlf. (07) 92 16 11
Oslokontor, Drammensveien 230, Oslo 2 - Tlf. (02) 55 31 65

Rapport nr. 86.042	ISSN 0800-3416	Åpen/~~Fortrolig til~~

Tittel:
On numerical AMT profiles and sounding curves over some two-dimensional structures

Forfatter:
Raimo Pelkonen

Oppdragsgiver:
NTNF

Fylke:

Kommune:

Kartbladnavn (M. 1:250 000)

Kartbladnr. og -navn (M. 1:50 000)

Forekomstens navn og koordinater:

Sidetall: 57 Pris: kr. 80,-

Kartbilag:

Feltarbeid utført:	Rapportdato: 07.03.1985	Prosjektnr.: 1765	Prosjektleder: Raimo Pelkonen

Sammendrag:

AMT apparent resistivity sounding curves have been calculated above some two-dimensional horizontal, dipping and vertical conductors in a host rock. The calculations have been made using a finite element computer program for plane wave modelling developed by the author. The curves have been calculated for both the tangential electric (TE) and tangential magnetic (TM) modes and they have been interpreted using a one-dimensional model in order to study what kind of one-dimensional interpretation these two-dimensional models give.

Emneord	Geofysikk	Modellforsøk
	Elektromagnetisk måling	Fagrapport

CONTENTS

PELKONEN, R., * 1985: ON NUMERICAL AMT PROFILES AND SOUNDING CURVES OVER SOME TWO-DIMENSIONAL STRUCTURES. Dept. of Geophysics, Univ. of Oulu, Report No. 11, 57 p.

ABSTRACT

AMT apparent resistivity sounding curves have been calculated above some two-dimensional horizontal, dipping and vertical conductors in a host rock. The calculations have been made using a finite element computer program for plane wave modelling developed by the author. The curves have been calculated for both the tangential electric (TE) and tangential magnetic (TM) modes and they have been interpreted using a one-dimensional model in order to study what kind of one-dimensional interpretation these two-dimensional models give.

When the two-dimensional conductor is horizontal at different depths (50-400 m) or dips from 0^{o} to 45^{o}, one-dimensional interpretation of TE-mode data locates the body well, although there are indications of the conductor beyond its edges because of induction effects. On the basis of the resistivity values of these indications we can, to some extent, locate the edges of the actual conductor. When the dip of the conductor exceeds 45^{o}, one-dimensional interpretation of TE-mode data is no longer reliable. When the conductor is horizontal and lies near the surface (depth $\leq$100 m) or dips from 0^{o} to 15^{o}, one-dimensional interpretation of TM-mode data indicates, because of current gathering, only the central part of the body and the interpreted conductances at this part are too high. When the conductor is horizontal and deep lying or dips more than 15^{o}, one-dimensional interpretation of TM-mode data does not indicate it at all.

On the basis of one-dimensional interpretation of TE-mode data over thin vertical two-dimensional conductors at different depths (100-1000 m) it is not possible to build up the actual model.

*Lapin Malmi, Kairatie 56, SF-96100 Rovaniemi 10, Finland; formerly at the Geological Survey of Norway, P.O. Box 3006, N-7001 Trondheim, Norway

INTRODUCTION

Scalar audiomagnetotelluric (AMT) sounding curves are usually interpreted using a layered earth model, i.e. one-dimensional model. Fournier (1970) has introduced a special nomogram for plotting magnetotelluric (MT) apparent resistivity sounding curves and on the basis of the depth and conductance lines of the nomogram rough one-dimensional interpretation can be performed. This nomogram is also used in this paper. The present discussion of MT is also valid to AMT because of scaling conditions of electromagnetic fields. Berdichevsky (1968) has shown, how extreme points of MT sounding curves can be used for the determination of depths to conductors and the total conductance of the layers above an insulator. Theoretical sounding curves over a layered model can be calculated analytically (Kunetz, 1972) with a pocket calculator or with a computer and there exist several computer programs for curve fitting between measured and theoretical data (e.g. Wu, 1968; Pelkonen et al., 1979). We can always use one-dimensional models for interpreting scalar AMT data, but since the structure is most often two or three-dimensional, we have difficulties in understanding what our one-dimensional interpretation means. This is why we have calculated theoretical AMT sounding curves over some two-dimensional conductors and interpreted the two-dimensional AMT data with a one-dimensional model in order to get experience of what kind of one-dimensional interpretation these two-dimensional structures give.

Although there exist papers on two and also on three-dimensional AMT or MT modelling, the most frequently used model in routine interpretation is still a one-dimensional model. This is due to the fact that theoretical AMT or MT anomalies over complicated structures have to be calculated using either analogue or numerical modelling and in routine work there is rarely time or equipment to do this. Most authors have shown only profiles with one or a few frequencies and one cannot construct sounding curves on the basis of these profiles. Porstendorfer (1975) and Adam

(1976) have reviewed MT work and the results of analogue and numerical modelling over some complicated structures. Tatrallyay (1977) has calculated numerically MT sounding curves over two-dimensional pinching and embedding horizontal conductors, while Kaikkonen (1983) has calculated AMT profiles and sounding curves over some two-dimensional dipping and vertical conductors, also numerically. Saksa (1983) has developed AMT nomograms over two-dimensional horizontal conductors based on numerical modelling. Hohmann and Ting (1978) and Wannamaker et al. (1984) have described the basics of their numerical methods for calculating MT responses over three-dimensional models and some examples calculated with their programs. Park et al. (1983) have shown some MT sounding curves over three-dimensional structures using numerical modelling.

Before showing the results of our two-dimensional AMT modelling, we shall present the computer program used for calculating AMT anomalies over two-dimensional conductive and/or permeable bodies.

COMPUTER PROGRAM

Finite element formulation

Andersen (1977) has developed a finite element program for two-dimensional calculation of eddy current problems in power engineering applications. The program can handle both flat and axi-symmetric fields. In flat fields, a Cartesian x,y,z coordinate system is used, and the field is constant in the z-direction. In axi-symmetric fields, a cylindrical r,z,θ coordinate system is used, and the field is constant in the tangential θ-direction. The flat field part of the program has been developed further for two-dimensional plane wave modelling. The computer program for two-dimensional Turam modelling described in Lile et al. (1982) was also based on the program of Andersen (1977).

We shall study eddy current problems, where the current density $\vec{J}_z$ is unidirectional and parallel to the strike of the two-dimensional inhomogeneity. Thus the currents flow perpendicular to the x,y plane. This is called the E-polarization or TE-mode (tangential electric). For sinusoidally varying fields of low enough frequency, so that displacement currents can be neglected, the diffusion equation which governs this eddy current problem is:

$$\nabla^2 \vec{A}_z = \mu\sigma(j\omega\vec{A}_z - \vec{U}_z) \tag{1}$$

where $\vec{A}_z$ = magnetic vector potential, μ = permeability, σ = conductivity, j = imaginary operator $\sqrt{-1}$, $\omega = 2\pi f$ = rotational frequency, f = frequency and $\vec{U}_z$ = curl free vector field. SI units are used throughout.

In the plane wave case there are no external sources and thus $\vec{U}_z = \vec{0}$. Equation 1 can then be written:

$$\frac{\partial^2 \vec{A}_z}{\partial x^2} + \frac{\partial^2 \vec{A}_z}{\partial y^2} - j\omega\mu\sigma\vec{A}_z = 0 \tag{2}$$

According to the finite element method, this equation can be solved by minimizing the corresponding energy functional:

$$\vec{W} = \iint_R \left\{ \frac{1}{2\mu} \left[\left(\frac{\partial \vec{A}_z}{\partial x} \right)^2 + \left(\frac{\partial \vec{A}_z}{\partial y} \right)^2 \right] + \frac{1}{2} j\omega\sigma\vec{A}_z \cdot \vec{A}_z \right\} dxdy \tag{3}$$

The field region R is covered with a grid consisting of triangular elements. The minimization of $\vec{W}$ implies that the partial derivatives of $\vec{W}$ with respect to the vector potentials at all the nodes in the grid should be zero. A linear variation of the vector potential is assumed within each triangle (constant flux density), and an equation can be derived giving the vector poten-

tial at a node as a linear function of the vector potentials at the surrounding nodes. The complete set of equations is solved directly by Gaussian elimination, and the result is the vector potential at every node in the grid.

Calculation by analogies

In some eddy current problems the current flow is in the x,y plane, and the flux density $\vec{B}_z$ is unidirectional and parallel to the strike of the two-dimensional inhomogeneity. This is called the H-polarization or TM-mode (tangential magnetic). Andersen (1982) has shown, how certain analogies in the basic field equations can be exploited to solve also this kind of problems with unidirectional flux density, using the same computer programs which have been developed for unidirectional current density. Some of these analogous equations and quantities are shown in Table 1.

Unidirectional flux density (TM-mode)	Unidirectional current density (TE-mode)
$\nabla\times\vec{H}_z = \vec{J}_{x,y}$	$\nabla\times\vec{A}_z = \vec{B}_{x,y}$
$\vec{J}_{x,y}$	$\vec{B}_{x,y}$
$\vec{H}_z$	$\vec{A}_z$
$\vec{J}_{x,y} = \sigma\vec{E}_{x,y}$	$\vec{B}_{x,y} = \mu\vec{H}_{x,y}$
$\vec{E}_{x,y}$	$\vec{H}_{x,y}$
σ	μ
$\int\vec{E}_{x,y}\vec{J}_{x,y}dv$	$\int\vec{H}_{x,y}\vec{B}_{x,y}dv$
$\nabla\times\vec{E}_{x,y} = -j\omega\vec{B}_z$	$\nabla\times\vec{H}_{x,y} = \vec{J}_z$
$-j\omega\vec{B}_z$	$\vec{J}_z$
$\vec{B}_z = \mu\vec{H}_z$	$\vec{J}_z = \sigma\vec{E}_z$
μ	σ
$-j\omega\vec{H}_z$	$\vec{E}_z\ (= -j\omega\vec{A}_z)$
$\omega^2\int\vec{H}_z\vec{B}_z dv$	$\int\vec{E}_z\vec{J}_z dv$

Table 1. Analogy between the cases with the unidirectional flux and current densities (Andersen, 1982).

$\vec{H}_z$	= magnetic field	$\vec{A}_z$	= vector potential
$\vec{J}_{x,y}$	= current density	$\vec{B}_{x,y}$	= flux density
$\vec{E}_{x,y}$	= electric field	$\vec{H}_{x,y}$	= magnetic field
$\vec{B}_z$	= flux density	$\vec{J}_z$	= current density
		$\vec{E}_z$	= electric field

The most important analogy is that flux density $\vec{B}_{x,y}$ in TE-mode corresponds to current density $\vec{J}_{x,y}$ in TM-mode. The depth of penetration (skin depth)

$$\delta = \sqrt{2/(\mu\omega\sigma)} \qquad (4)$$

is naturally kept unchanged.

Andersen (1982) has described how the input of his program (Andersen, 1977) has to be changed in order to calculate cases where the flux density is unidirectional, and how the output in this case is to be interpreted. In the program described here no changes are needed, because they are programmed.

If we change the quantities in Equations 1-3 according to Table 1, similar equations can be derived for the case where the flux density is unidirectional. The energy functional becomes a function of the magnetic field $\vec{H}_z$, and the result of the finite element analysis is the magnetic field at every node in the grid.

Additional operations

In the plane wave case we are interested in AMT and we need the apparent resistivity ρ_a and the phase angle ϕ between horizontal electric and magnetic fields. In TE-mode (unidirectional current density) these are:

$$\rho_a = \frac{1}{\omega\mu}\left(\frac{|\vec{E}_z|}{|\vec{H}_x|}\right)^2 \qquad (5)$$

$$\phi = \measuredangle \vec{E}_z - \measuredangle \vec{H}_x - \pi$$

and in TM-mode (unidirectional flux density) with $\sphericalangle \vec{H}_z = \pi$:

$$\rho_a = \frac{1}{\omega\mu}\left(\frac{|\vec{E}_x|}{|\vec{H}_z|}\right)^2 \qquad (6)$$

$$\phi = \sphericalangle \vec{E}_x$$

In TE-mode the electric field is $-j\omega$ times the vector potential (Table 1), while the magnetic field is calculated from the vector potentials by numerical differentiation.

In TM-mode the electric field is calculated by numerical differentiation of the magnetic field (Table 1), while the magnetic field is constant on the surface of the ground.

Use of the program

Figs. 1a and 2a show the main characteristics of the problem region. The calculations are made in a rectangular area. In TE-mode (Fig. 1a) the region consists of air, half-space and anomalous conductor(s). The vector potential is set to a constant on the top of the air, vanishing at the bottom of the half-space. In TM-mode (Fig. 2a) the region consists of the half-space and anomalous conductor(s). The magnetic field is set to a constant on the surface of the ground, vanishing at the bottom of the half-space. The top of the air in TE-mode and the bottom of the half-space in both the modes are at a distance of 3-4 times the skin depth of the half-space from the surface of the ground. In both the modes the sides of the problem region are at a distance of 3-4 times the skin depth of the half-space from the nearest lateral conductivity contrast. The distances mentioned here depend somewhat on the actual problem, but in any case they should not be smaller.

The computer program uses automatic grid generation, the principles of which are described in Andersen (1973). The user decides only on an initial grid made up of horizontal and vertical lines (through the tic-marks in Figs. 1a and 2a), which divide the field region up into a rectangular grid. Then the program makes this rectangular grid into a triangular grid, which fits the contours of interfaces between different materials. The program permits considerable flexibility in the spacing of the grid lines, so the mesh sizes can be varied according to the requirements, with the finest meshes in the regions where the flux and current densities change most rapidly.

Contours of different materials are specified as a series of coordinates which are joined by straight line segments by the program. Certain shapes (rectangular, parallellogram and circular bodies) are preprogrammed and can be specified in a simplified manner.

Figs. 1-2 are typical output of the program. Fig. 1 shows the plot of flux lines and the TE-mode apparent resistivity and phase angle profiles over a model. Fig. 2 shows the plot of current flow lines and the TM-mode apparent resistivity and phase angle profiles over the same model as in Fig. 1.

Program characteristics

The program is written in Fortran IV for the Univac 1100/62 computer of the Norwegian Institute of Technology. It occupies 79 kilowords in the central processor and requires 156 kilowords of auxiliary storage. The maximum number of nodes is 1650.

The program is also converted to the Hewlett-Packard 3000 series III computer of the Geological Survey of Norway, and is enlarged, so that the maximum number of nodes is 3100. The calculation of

the TE-mode example of Fig. 1 with 1645 nodes requires computing time on the Univac about 2 minutes, while the TM-mode example of Fig. 2 with 1222 nodes about 1 minute. The computing times on the Hewlett-Packard are about 50 and 25 minutes, respectively.

Also the Hewlett-Packard version of the computer program for Turam modelling described in Lile et al. (1982) is enlarged, so that the maximum number of nodes is 3100. Then with the Hewlett-Packard versions we can study the anomalies over more complicated models than with the Univac versions, because the more complicated the model, the more node points we need in order to solve the case. The number of nodes in the Univac versions can certainly be enlarged, too.

TWO-DIMENSIONAL AMT MODELLING

Models

We have studied different kinds of two-dimensional conductors in a host rock. In Model 1 (Fig. 3) the conductor is horizontal, it is 400 m wide, 10 m thick, the conductance is 5 S, and the depth from the ground is varied from 50 to 400 m. In Model 2 (Fig. 4) the conductor dips, the top of it being at a depth of 10 m. It is 400 m long, the conductance is 20 S, and the dip angle is varied from 15 to 90°. In Model 3 (Fig. 5) the conductor is vertical, it is 25 m thick, 500 m long, the conductance is 10 S, and the depth from the ground is varied from 100 to 1000 m. The resistivity of the host rock is 5000 Ωm in all the models.

We have first calculated AMT profiles over the models for both the TE and TM-mode. The profiles are the apparent resistivity and the phase angle between horizontal electric and magnetic fields, perpendicular to each other. In Model 1 we used ten frequencies from 17000 to 8 Hz, and six different grids (grid 1 for 17000 Hz, grid 2 for 3700 and 1700 Hz, grid 3 for 800 and

370 Hz, grid 4 for 170 and 80 Hz, grid 5 for 37 and 17 Hz and grid 6 for 8 Hz) for each depth. In Models 2 and 3 we used nine frequencies from 3700 to 8 Hz, and five different grids for each dip in Model 2, and five different grids for each depth in Model 3. The frequency band is the same that the French AMT equipment ECA 541-0 manufactured by Societe ECA (Benderitter et al., 1973) operates with, and in Model 1 we have included a VLF frequency. The calculations have been made with the Hewlett-Packard computer program described in the previous chapter, the number of node points in every grid being about 1650 for Model 1, and about 3000 for Models 2 and 3. To obtain the apparent resistivity and phase angle profiles for one frequency the computing time was about 50 minutes for TE-mode and about 25 minutes for TM-mode in Model 1, about 1½ hours for TE-mode in Models 2 and 3 and about 1 hour for TM-mode in Model 2.

From the AMT profiles at different frequencies a program constructed apparent resistivity and phase angle sounding curves at different coordinates of the profile. We have studied only the apparent resistivity sounding curves which have been interpreted with an interactive computer program (Pelkonen et al., 1979) using a layered earth model, i.e. a one-dimensional model.

In the following we shall discuss the results model by model. The results of AMT modelling over Models 2 and 3 were briefly discussed by Carstens and Pelkonen (1983).

Results of Model 1

Figs. 6-10 show the apparent resistivity and phase angle profiles over Model 1, when the conductor is at depths of 50, 100, 200, 300 and 400 m, respectively. The profiles are drawn with the frequencies 17000, 3700, 800, 170, 37 and 8 Hz, and they are symmetrical with respect to the coordinate 0 m. In the following we

shall study the apparent resistivity and phase angle profiles together. Because of induction effects the TE-mode profiles have a tendency to broaden over the edge of the conductor. The anomalies in the TE-mode profiles are clear except in the profiles of the VLF frequency 17000 Hz, when the conductor is at a depth of 400 m. In this case there are no anomalies, because the conductor is too deep compared with the skin depth at 17000 Hz (273 m). Because of current gathering the TM-mode profiles are sharp and they indicate only the central part of the near surface conductor. The effect of the conductor is very clear in all the TM-mode profiles, when the conductor is at a depth of 50-200 m. When the depth is 300 m or greater, the anomalies in the TM-mode are quite poor.

The apparent resistivity sounding curves over Model 1 and their one-dimensional interpretations are in Figs. 11-18. When the conductor is at a depth of 50-200 m, the sounding curves of both the modes are shown. When the conductor is lying deeper, only the TE-mode curves are shown. The TE-mode curves are drawn at the coordinates 0-800 m, while the TM-mode ones are at the coordinates 0-150 m. The depth and conductance lines belonging to the two-dimensional conductor are marked in the nomograms. Also the theoretical one-dimensional sounding curves corresponding to the two-dimensional models are drawn. In the one-dimensional model the conductor is enlarged to a layer and one-dimensional AMT anomaly was calculated analytically with a program described by Pelkonen et al. (1979).

In the interpretations also the actual conductors are drawn and this is why it is easy to compare one-dimensional interpretation with the real structure. Resistivity and/or conductance values of the interpreted conducting layers are written in the interpretations.

All the TE-mode curves are three-layer curves of type H and one-dimensional interpretation of them locates the two-dimensional conductor well at all the depths, but because of induction

effects there are indications of the conductor beyond the edges of it. The true conductance is not achieved. The interpreted indications can be classified on the basis of the resistivities more easily than on the basis of their conductances. In these examples they are classified as good ($\rho \leqq 30$ Ωm), medium ($30 < \rho \leqq 100$ Ωm) or poor ($100 < \rho \leqq 300$ Ωm) and then, on the basis of these classified indications, we can build up the actual conductors well enough for practical purposes. However, the classification of indications found in field measurements is not as easy as in these theoretical examples.

The TM-mode sounding curves are two-layer curves, but they have been interpreted using a three-layer model, if possible, in order to find out the conductances of the conducting layers. When the two-dimensional conductor is at a depth of 50 m, one-dimensional interpretation locates only the central part of it at the coordinates 0-100 m. The conductances are greater than the true value. The sounding curves at the coordinates 150-800 m (the curves at the coordinates 200-800 m are not drawn) do not at all indicate the conductor. This is due to current gathering: with the frequencies used, most of the current gathers at the centre of the conductor and no information is obtained from the structure under it or outside it. When the conductor is at a depth of 100 m, there are poor indications of the conductor at the coordinates 0-50 m. When the conductor is at a depth of 200 m or greater, TM-mode sounding curves do not indicate it at all. However, in the TM-mode profiles with h=200 m (Fig. 8) there are clear anomalies, but here we study only the apparent resistivity curves and thus lose information.

We can conclude that one-dimensional interpretation of TE-mode data over horizontal two-dimensional conductors gives correct depth estimates, but it is difficult to locate the edges. However, by classifying the interpreted indications, the edges can be located well enough for practical purposes. One-dimensional interpretation of TM-mode data over near surface horizontal two-dimensional conductors gives correct depth estimates, but too high conductances at the centre of the actual conductor.

Results of Model 2

Figs. 19-24 show the apparent resistivity and phase angle profiles of both the modes over Model 2, when the conductor dips at 15, 45 and 90°. The profiles are drawn with the frequencies 3700, 800, 170, 37 and 8 Hz. In the following we shall study the apparent resistivity and phase angle profiles together. Again because of induction effects the TE-mode profiles have a tendency to broaden over the edges of the conductor. The effect of the conductor is very clear in all the TE-mode profiles, and the top of the conductor and its dip direction can be determined on the basis of these profiles. Because of current gathering the TM-mode profiles are sharp and they indicate only the top and the central part of the conductor. The dip direction can be determined also on the basis of the TM-mode profiles. When the conductor dips at 90°, the apparent resistivity anomalies are very narrow and the phase angle profiles have no anomalies at all.

The apparent resistivity sounding curves over Model 2 and their one-dimensional interpretations are shown in Figs. 25-29. When the conductor dips at 15 and 45°, the sounding curves at both the modes are shown: the TE-mode curves at the coordinates -500-1000 m, and the TM-mode ones at the coordinates 0-300 m. When the conductor dips at 90°, only the TE-mode curves are shown and they are drawn at the coordinates 0-1000 m. The conductance line belonging to the two-dimensional conductor is marked on the nomograms.

When the conductor dips at 15 or 45°, the TE-mode sounding curves are three-layer curves of type H in spite of the curves at the coordinates 0 and -50 m for the dip 15° and at the coordinate 0 m for the dip 45°. At these coordinates the interpreted conductor is at the surface. One-dimensional interpretation locates the two-dimensional conductor well for both the dips, although we have indications of the conductor beyond the edges of it. The true conductance is not achieved. On the basis of the resisti-

vity values of the indications we can classify them as good ($\rho \leqq 30$ Ωm), medium ($30 < \rho \leqq 100$ Ωm) or poor ($100 < \rho \leqq 300$ Ωm). On the basis of these classified indications the actual conductor can then be built up well enough for practical purposes for the dip 15°. When the dip is 45° there is a little more uncertainty in the interpretation.

When the conductor dips at 90°, the case is symmetrical with respect to the coordinate 0 m. The TE-mode sounding curves are three-layer curves of type H in spite of the curve at the coordinate 0 m, where the interpreted conductor is at the surface. In this case one-dimensional interpretation does not locate the conductor, it only indicates conducting layers beyond it. The true conductance is not achieved. By classifying the indications as good, medium or poor, we can restrict the anomalous area, but we cannot build up the actual model. We can only say that there is a conductor with a dip between 45 and 135°.

When the conductor dips at 15°, the TM-mode sounding curves are two-layer curves but they have been interpreted using a three-layer model, if possible, in order to find out the conductances of the conducting layers. One-dimensional interpretation locates the two-dimensional conductor well, but it indicates only a part of it. The rest of it is so deep that TM-mode does not see it. The conductances are too great the highest being 500 S. The curves at the coordinates 0-200 m do not at all indicate the high-resistance layer under the true conductor. This is again due to current gathering: with the frequencies used, most of the current gathers at the top and central part of the conductor and no information is obtained from the structure under it or outside it.

When the conductor dips at 45°, the TM-mode sounding curves do not indicate the conductor and this is why they have not been interpreted.

We can conclude that when a two-dimensional conductor dips at even 45°, one-dimensional interpretation of TE-mode data locates it satisfactorily. When the dip exceeds 45°, we cannot achieve a reliable one-dimensional interpretation. One-dimensional interpretation of TM-mode data over two-dimensional slightly dipping conductors gives correct depth estimates but too high conductances at the central part of the actual conductor.

Results of Model 3

Figs. 30-31 show the TE-mode apparent resistivity and phase angle profiles over Model 3, when the top of the conductor is at depths of 100, 250, 500 and 1000 m. The TM-mode profiles are not shown, because they have no anomalies. The profiles are drawn with the frequencies 3700, 800, 170, 37 and 8 Hz and they are symmetrical with respect to the coordinate 0 m. When studying the apparent resistivity and phase angle profiles together, we note that when the conductor is at a depth of 100-500 m, the anomalies are clear. When the conductor is at a depth of 1000 m, there are hardly anomalies at all.

The apparent resistivity sounding curves over Model 3 and their one-dimensional interpretations are shown in Figs. 32-35. The sounding curves are drawn only at the coordinates 0, 250, 500, 750 and 1000 m. The depth and conductance lines belonging to the two-dimensional conductor are drawn in the nomograms. When the two-dimensional conductor is at a depth of 100-500 m, one-dimensional interpretation over the conductor locates it somewhat deeper and indicates conducting layers beyond it. On the basis of the resistivity values of the indications we can restrict the anomalous area, but we cannot build up the actual model. The interpretation only shows an antiformal structure with the smallest resistivity value at its top, and we cannot determine if the structure is vertical or gently dipping.

When the conductor is at a depth of 1000 m, one-dimensional interpretation gives very poor indications of a nearly horizontal structure.

On the basis of the previous modelling it seems that we get clear indications of vertical two-dimensional conductors situated even at a depth of 500 m by using one-dimensional interpretation. The problem is, that we cannot build up vertical models on the basis of these indications. The interpreted antiformal structures from deep lying vertical conductors are similar to those of more flat-lying conductors. However, other information is generally available to help us to build up the most appropriate model.

Scaling condition

In the previous chapters we have presented AMT profiles and sounding curves at certain frequencies over certain models. The results can be scaled to correspond to other situations according to the scaling condition of electromagnetic fields:

$$\sigma_1 \mu_1 f_1 L_1^2 = \sigma_2 \mu_2 f_2 L_2^2, \qquad (7)$$

where the subscripts 1 and 2 refer to situations 1 and 2, and L=linear dimension. For instance the apparent resistivity and phase angle profiles of 3700 Hz over Models 2 and 3 correspond to the profiles of the VLF frequency 14800 Hz, if the linear dimensions in the Models 2 and 3 are divided by 2. Thus the results we have shown can be used e.g. to study VLF-R profiles over dipping and vertical conductors.

CONCLUSIONS

We have calculated AMT apparent resistivity and phase angle profiles and sounding curves over some two-dimensional horizontal, dipping and vertical conductors in a host rock. The calculations have been made with the described finite element computer program for plane wave modelling. The apparent resistivity sounding curves over these two-dimensional structures have been interpreted using a one-dimensional model. It must be emphasized that this AMT modelling would not have been practicable without the possibility of building the grids needed in the finite element calculations automatically.

We have concluded that when a two-dimensional conductor is horizontal at different depths (50-400 m) or dips at up to 45°, one-dimensional interpretation of TE-mode data locates the body well, although because of induction effects there are indications of the conductor beyond the edges of it. By classifying the resistivity values of these indications we can, to some extent, locate the edges of the actual conductor. When the dip of the conductor exceeds 45°, we cannot, on the basis of one-dimensional interpretation of TE-mode data, build up the actual model.

When the two-dimensional conductor is horizontal and lying near the surface (depth $\leqq$100 m) or dips at up to 15°, one-dimensional interpretation of TM-mode data indicates, because of current gathering, only the central part of it and the interpreted conductances at this part are too high. When the conductor is horizontal and deep lying or dips at more than 15°, one-dimensional interpretation of TM-mode data does not indicate it at all.

AMT field measurements also confirm that gently dipping conductors can reliably be followed by using one-dimensional interpretation (Carstens, 1979; Pelkonen et al., 1979; Pietilä and Hattula, 1982).

We have also concluded that we get clear indications of vertical two-dimensional conductors situated even at a depth of 500 m by using one-dimensional interpretation, but we cannot construct the actual model on the basis of these indications.

ACKNOWLEDGEMENTS

The development of the computer program was carried out in co-operation with Dr. Andersen of the Norwegian Institute of Technology while the author worked at the Geological Survey of Norway in a research project financed by the Royal Norwegian Council for Scientific and Industrial Research. The two-dimensional modelling and one-dimensional interpretation of the AMT data was made while the author worked on this research project. The report was written at a later stage. The author wishes to thank Dir. Aalstad of the Geophysics Division of the Geological Survey of Norway and Dr. Lile from the Norwegian Institute of Technology for support and valuable discussions during the research project.

The author wishes also to thank Dr. Boyd of the Geology Division of the Geological Survey of Norway for kindly checking the language of the paper.

REFERENCES

Adam, A. (editor), 1976: Geoelectric and geothermal studies. Akademiai Kiado, Budapest, 751 p.

Andersen, O.W., 1973: Laplacian electrostatic field calculations by finite elements with automatic grid generation. IEEE Transactions, PAS-92, 1485-1492.

Andersen, O.W., 1977: Finite element solution of skin effect and eddy current problems. IEEE Paper A77 615-8, Mexico City.

Andersen, O.W., 1982: Personal communication.

Benderitter, Y., Thach, H.N. and Jolivet, A., 1973: Magneto-telluric method for mining exploration. Paper presented at the 35th EAEG meeting in Brighton in June 1973, 27 p.

Berdichevsky, M.N., 1968: Electrical prospecting by the magneto-telluric method (in Russian). Nedra, Moscow, 255 p.

Carstens, C.W., 1979: Audio-magnetotelluric testmeasurements to ore exploration. Abstract of the paper presented at the 41st EAEG meeting in Hamburg in May-June 1979.

Carstens, C.W. and Pelkonen, R., 1983: Some case histories from deep ore exploration with the AMT method. Abstract of the paper presented at the 45th EAEG meeting in Oslo in June 1983.

Fournier, H.G., 1970: Contribution au développement de la méthode magnetotellurique, notamment en vue de la détermination des structures profondes. Ph.D. thesis, parts I, II and III. University of Paris, 122, 136 and 18 p.

Hohmann, G.W. and Ting, S.C., 1978: Three-dimensional magneto-telluric modeling. Final Report 77-15, Earth Science Laboratory, University of Utah Research Institute, Salt Lake City, Utah, 48 p.

Kaikkonen, P., 1983: Two-dimensional finite element modelling in magnetotellurics. Pp. 79-106 in The development of the deep geoelectric model of the Baltic Shield. Part 1. Numerical methods (editors Hjelt, S.E. and Vanyan, L.L.). Department of Geophysics, University of Oulu, Report No. 7.

Kunetz, G., 1972: Processing and interpretation of magnetotelluric soundings. Geophysics, 37, 6, 1005-1021.

Lile, O.B., Pelkonen, R., Andersen, O.W. and Singsaas, P., 1982: On the importance of gathered current in Turam measurements. Geoexploration, 19, 277-295.

Park, S.K., Orange, A.S. and Madden, T.R., 1983: Effects on three-dimensional structure on magnetotelluric sounding curves. Geophysics, 48, 1, 1402-1405.

Pelkonen, R., Hjelt, S.E., Kaikkonen, P., Pernu, T. and Ruotsalainen, A., 1979: On the applicability of the audiomagnetotelluric (AMT) method for ore prospecting in Finland. Department of Geophysics, University of Oulu, Contribution No. 94, 25 p.

Pietilä, R. and Hattula, A., 1982: An application of audiofrequency magnetotellurics and charge-potential method in skarn iron ore prospecting in the Rautuvaara area, Northern Finland. Abstract of the paper presented at the 44th EAEG meeting in Cannes in June 1982.

Porstendorfer, G., 1975: Principles of magnetotelluric prospecting. Gebrüder Borntraeger, Horb, 118 p.

Saksa, P., 1983: On electromagnetic source fields and their application to the audiomagnetotelluric method (in Finnish). Diploma engineering thesis, Technical University of Helsinki, 89+14 p.

Tatrallyay, M., 1977: On the interpretation of EM sounding curves by numerical modelling using the S.O.R. method. Acta Geodaetica, Geophysica et Montanistica, Academia Scientiarum Hungarica, 12, 279-285.

Wannamaker, P.E., Hohmann, G.W. and SanFilipo, W.A., 1984: Electromagnetic modeling of three-dimensional bodies in layered earths using integral equations. Geophysics, 49, 1, 60-74.

Wu, F.T., 1968: The inverse problem of magnetotelluric sounding. Geophysics, 33, 6, 972-979.

CAPTION FOR FIGS. 11-18, 25-29 AND 32-35

AMT sounding curves over Models 1 (Figs. 11-18), 2 (Figs. 25-29) and 3 (Figs. 32-35) and one-dimensional interpretations of them.

O M = coordinate (m) of the sounding curve
1-D = one-dimensional sounding curve corresponding to the actual model

10 M, 100 depth lines (m)
1 S, 10, 100, 1000 conductance lines (S)
the dotted depth lines are for 2,5,20,50,200 and 500 m and the dotted conductance lines for 2,5,20,50,200 and 500 S

100 M, 1000 depth lines (m)
.1 S, 1, 10, 100 conductance lines (S)
the dotted depth lines are for 20,50,200,500,2000 and 5000 m and the dotted conductance lines for .2,.5,2,5,20 and 50 S

50 / (5) depth line (m)/conductance line (S) belonging to the two-dimensional conductor

T positions
$\rho_i/\Omega m$ resistivities
$\sigma_i t_i/S$ conductances
} of the interpreted conducting layers

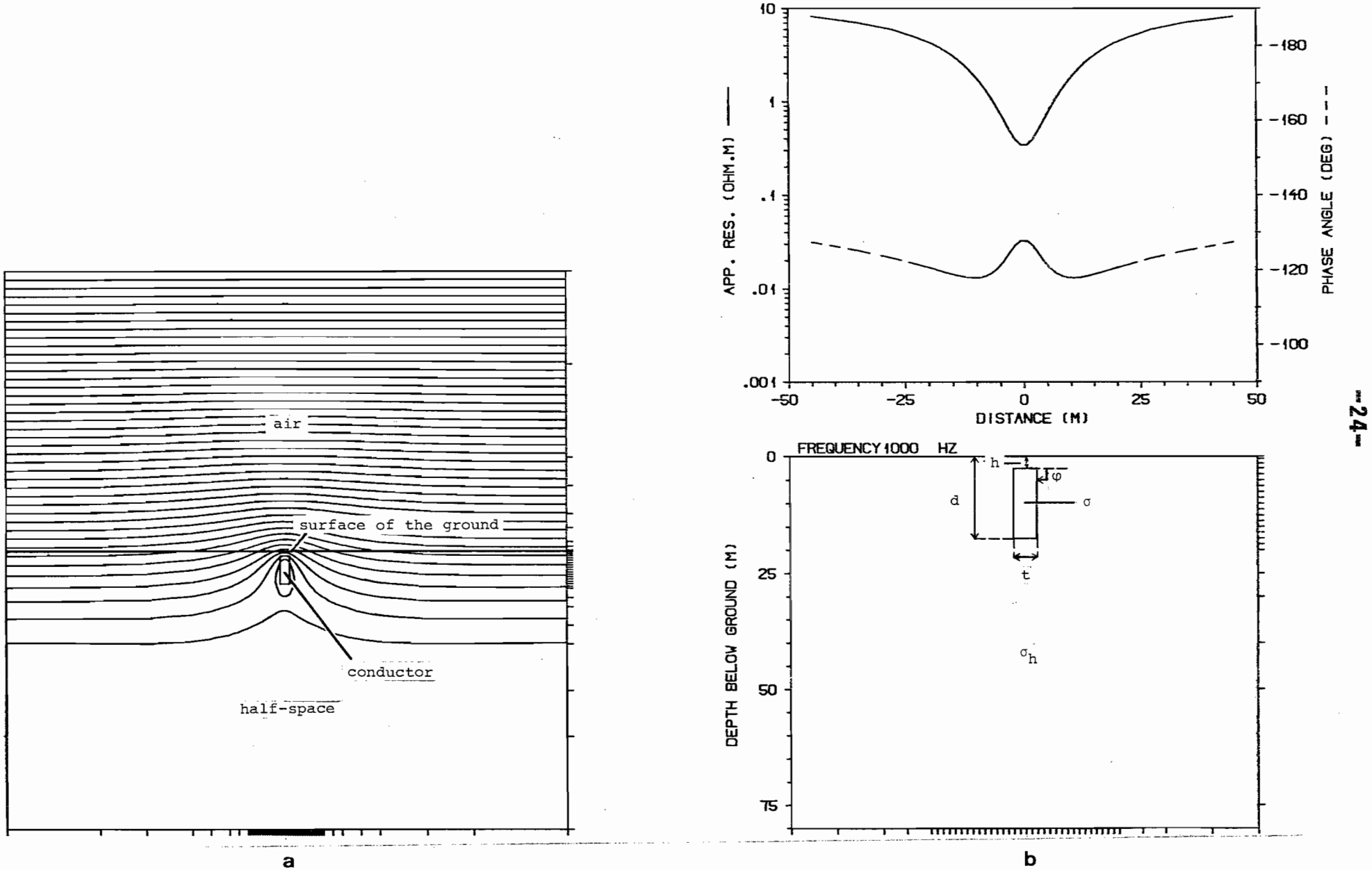

Fig. 1. The plot of flux lines (a) and the TE-mode apparent resistivity and phase angle profiles (b) over a model with a frequency of f=1000 Hz. The model parameters are φ=90°, h=2.5 m, d=17.5 m, t=5.0 m, σ=20.0 S/m and σ_h=0.1 S/m.

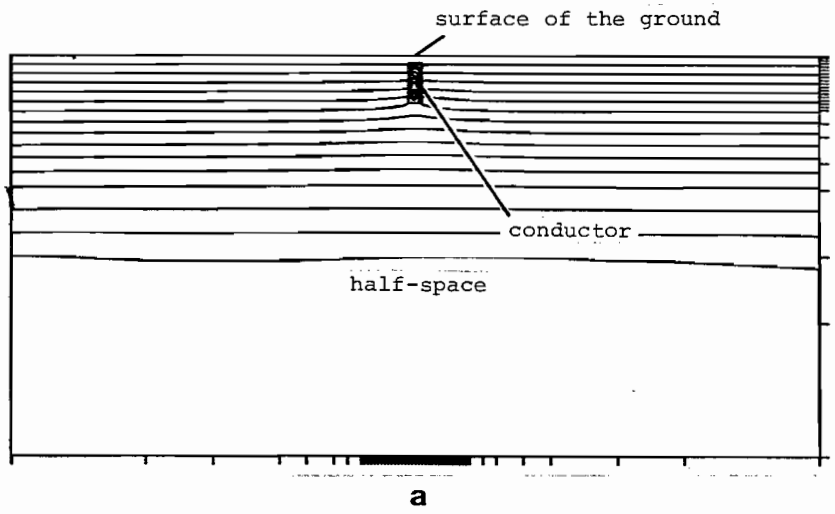

a

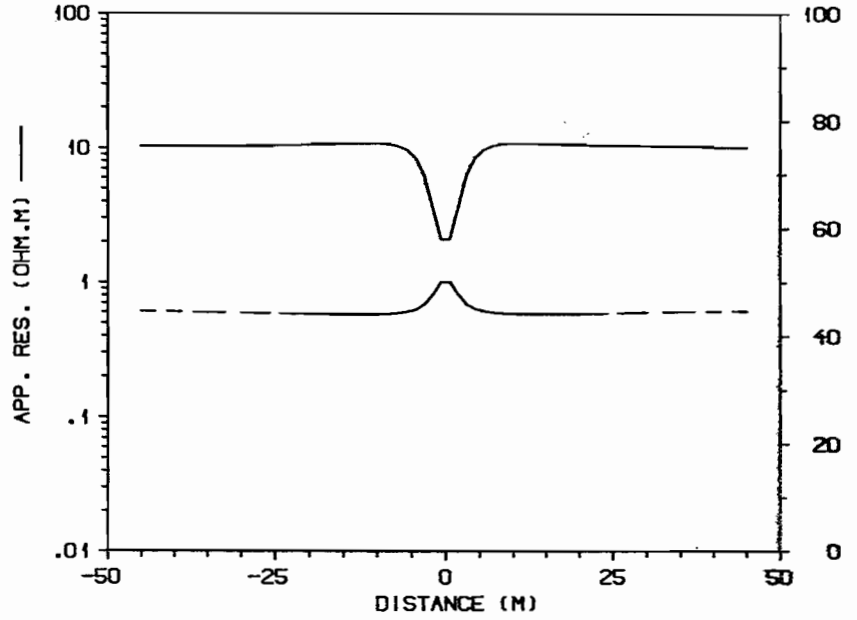

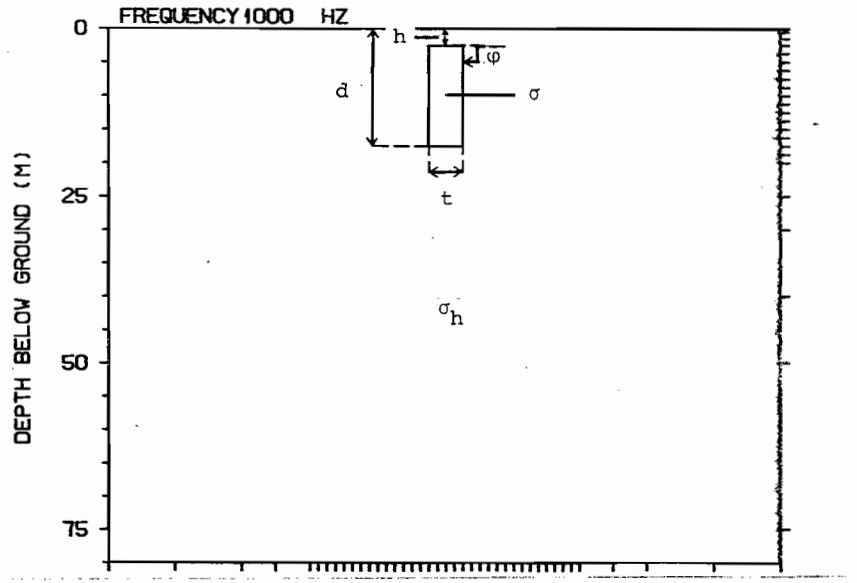

b

Fig. 2. The plot of current flow lines (a) and the TM-mode apparent resistivity and phase angle profiles (b) over a model with a frequency of f=1000 Hz. The model parameters are the same as in Fig. 1.

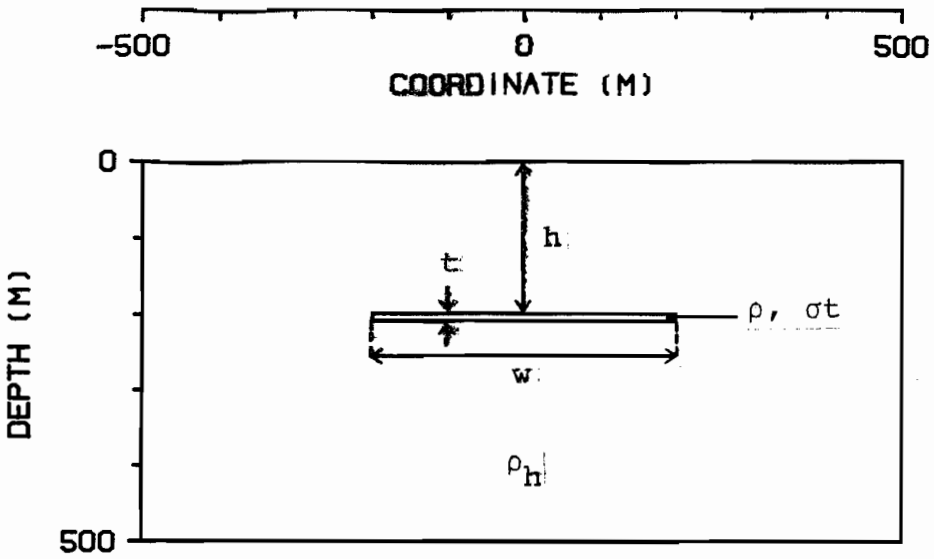

Fig. 3. Model 1: horizontal conductor in a host rock, h=50-400 m, w=400 m, t=10 m, ρ=2 Ωm, σt=5 S, ρ_h=5000 Ωm.

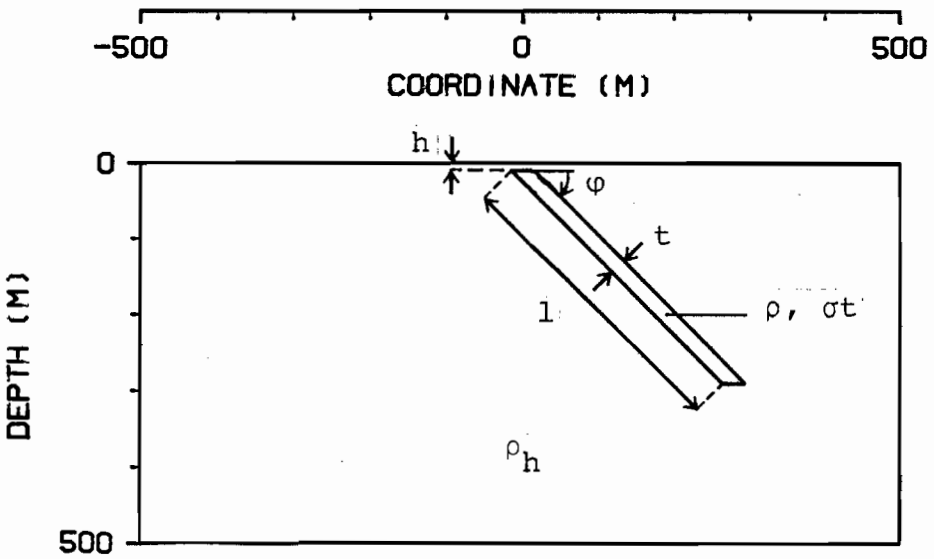

Fig. 4. Model 2: dipping conductor in a host rock, h=10 m, l=400 m, φ=15-90°, t=20 m, ρ=1 Ωm, σt=20 S, ρ_h=5000 Ωm.

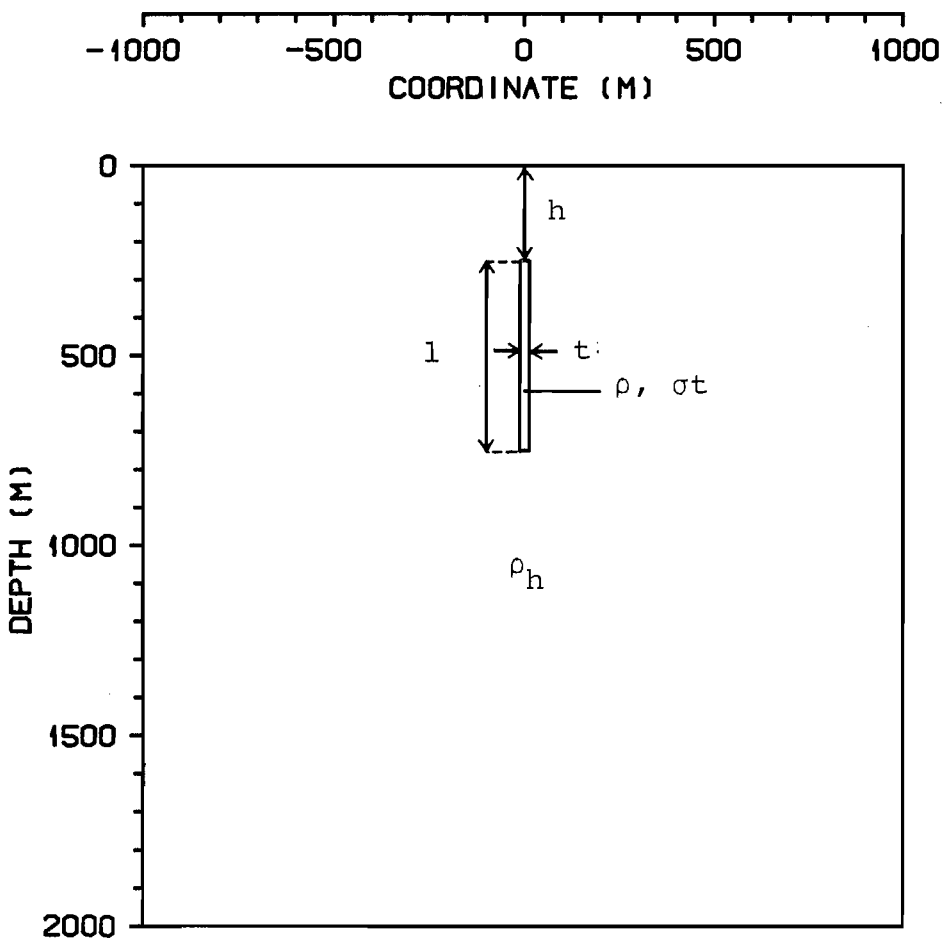

Fig. 5. Model 3: vertical conductor in a host rock, h=100-1000 m, l=500 m, t=25 m, ρ=2.5 Ωm, σt=10 S, ρ_h=5000 Ωm.

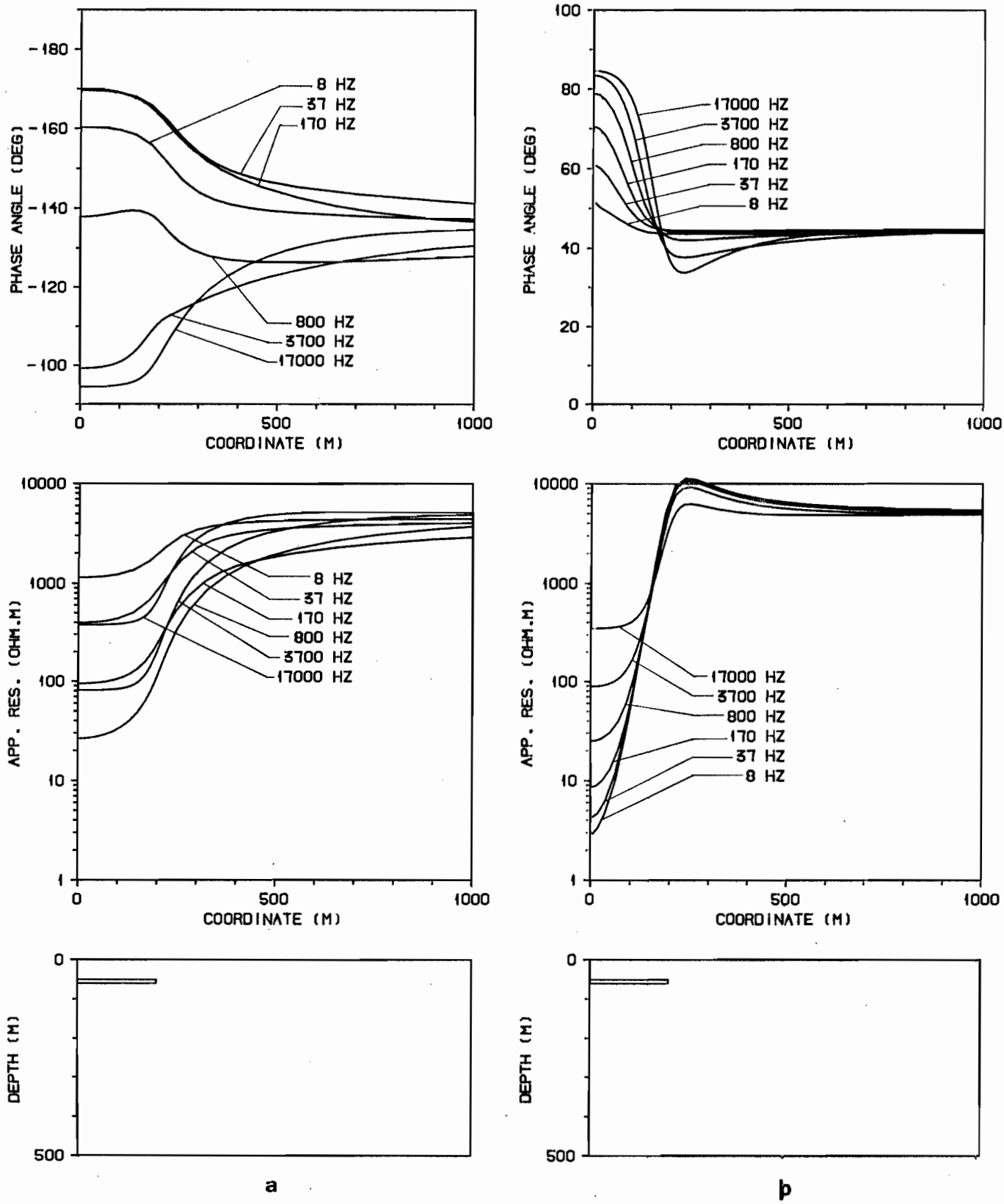

Fig. 6. AMT profiles of TE (a) and TM-mode (b) over Model 1 with h=50 m.

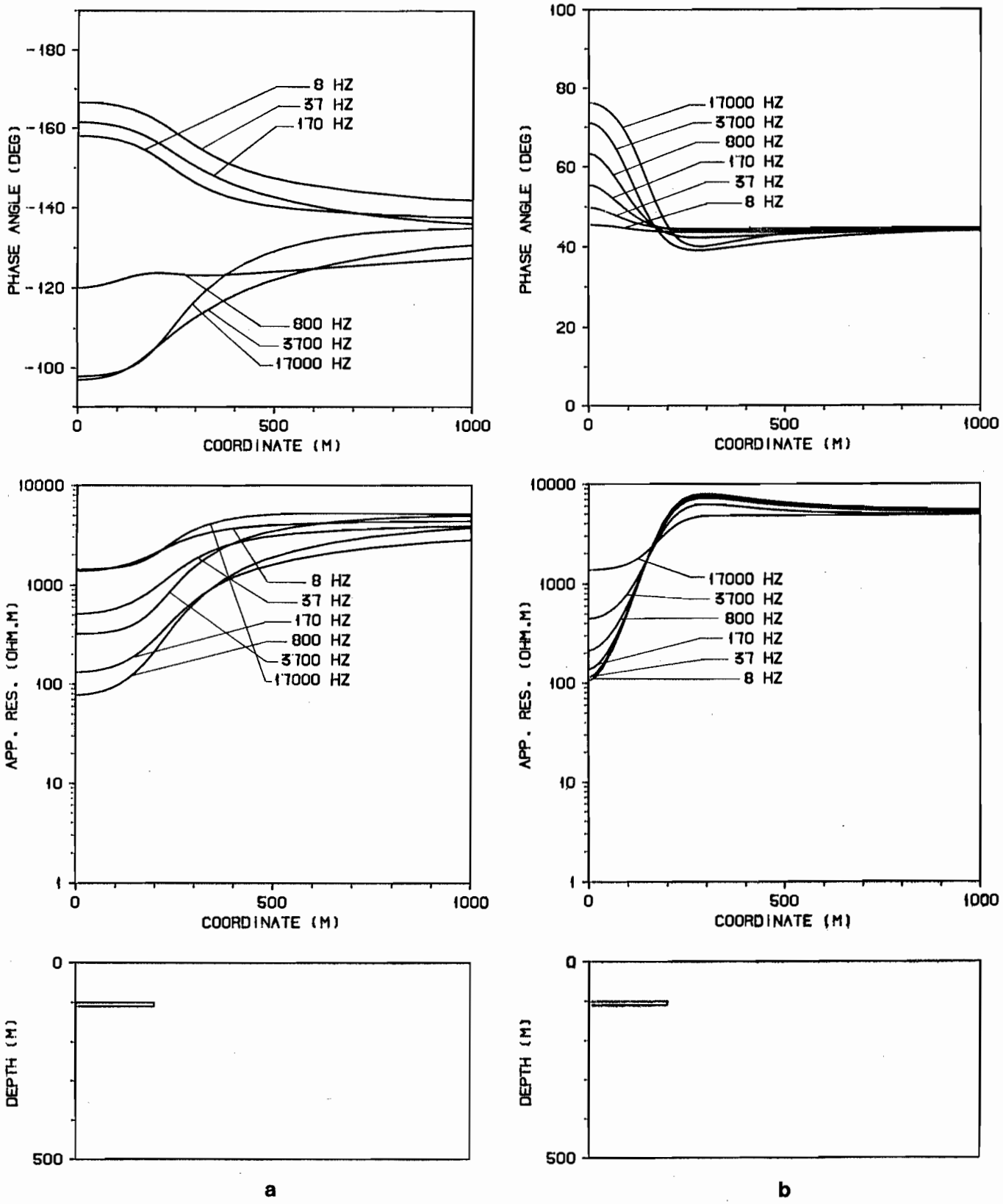

Fig. 7. AMT profiles of TE (a) and TM-mode (b) over Model 1 with h=100 m.

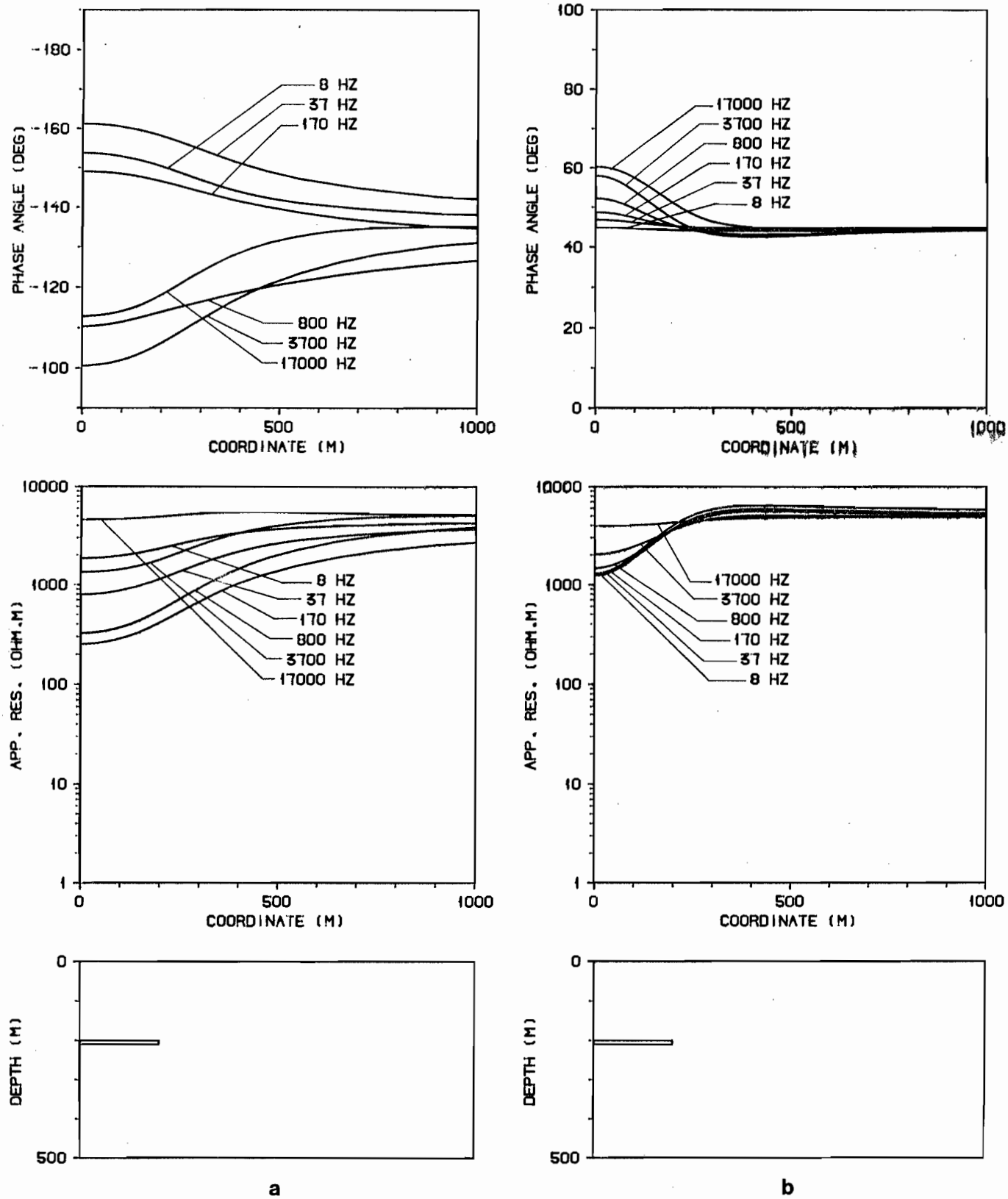

Fig. 8. AMT profiles of TE (a) and TM-mode (b) over Model 1 with h=200 m.

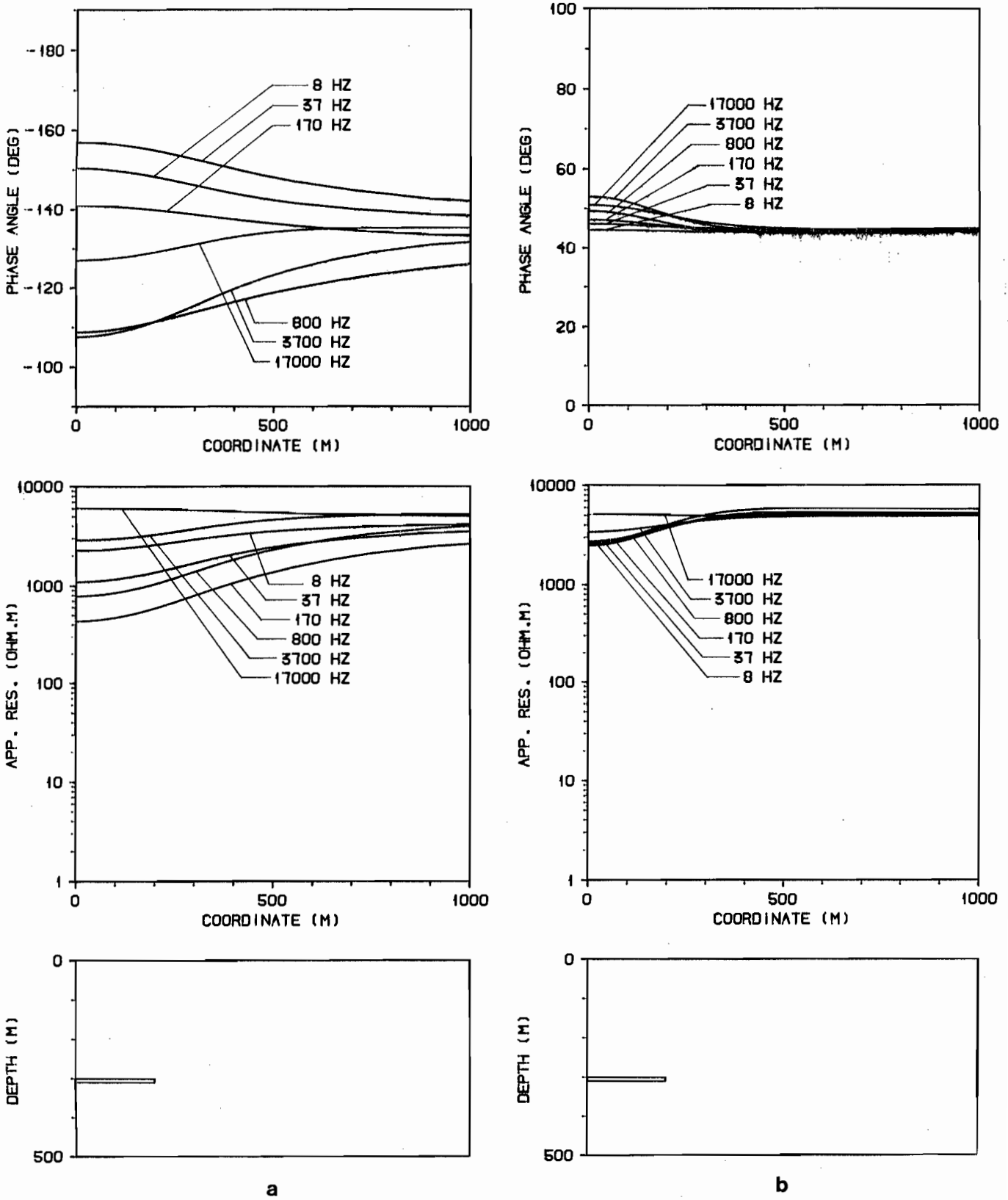

Fig. 9. AMT profiles of TE (a) and TM-mode (b) over Model 1 with h=300 m.

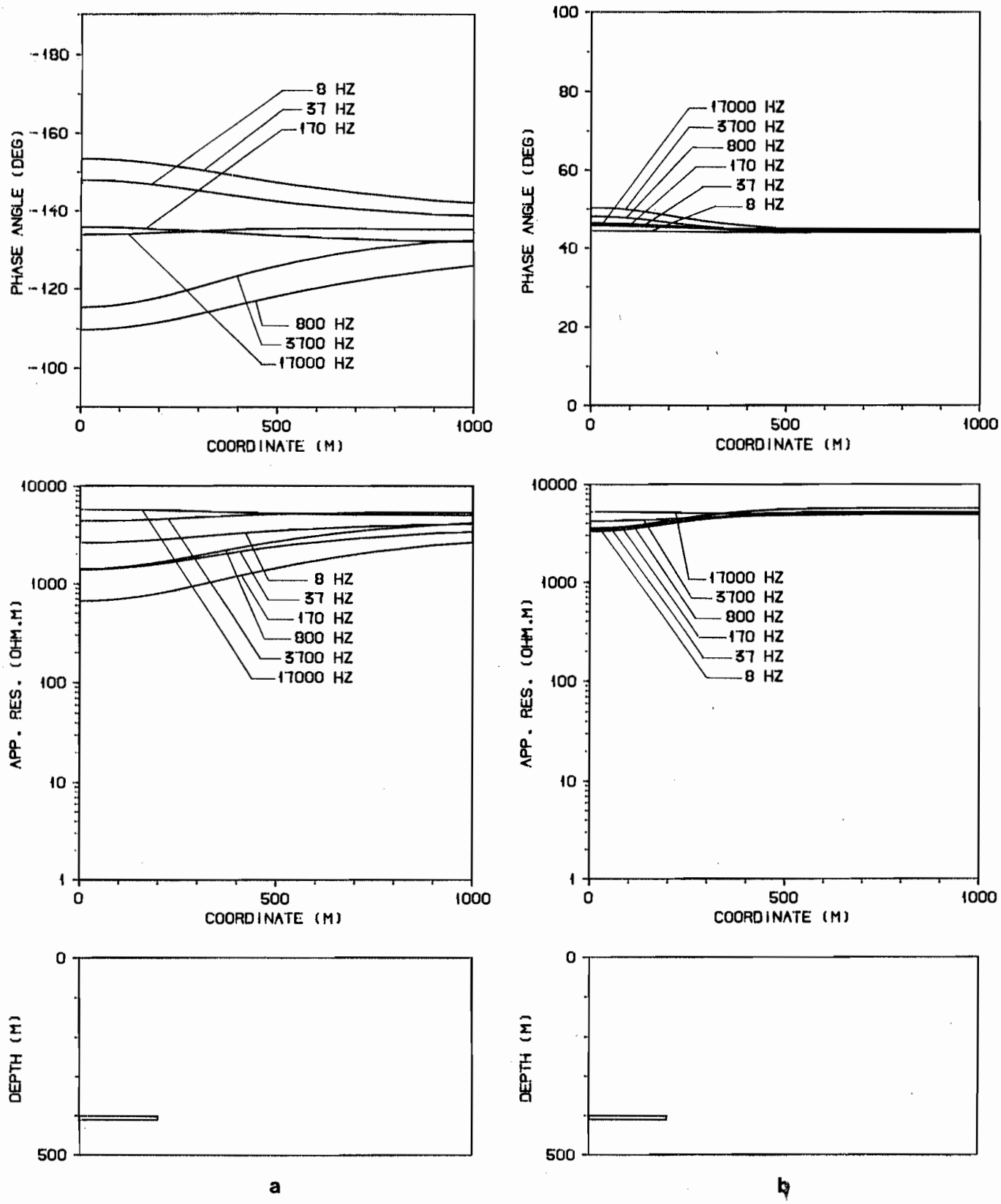

Fig. 10. AMT profiles of TE (a) and TM-mode (b) over Model 1 with h=400 m.

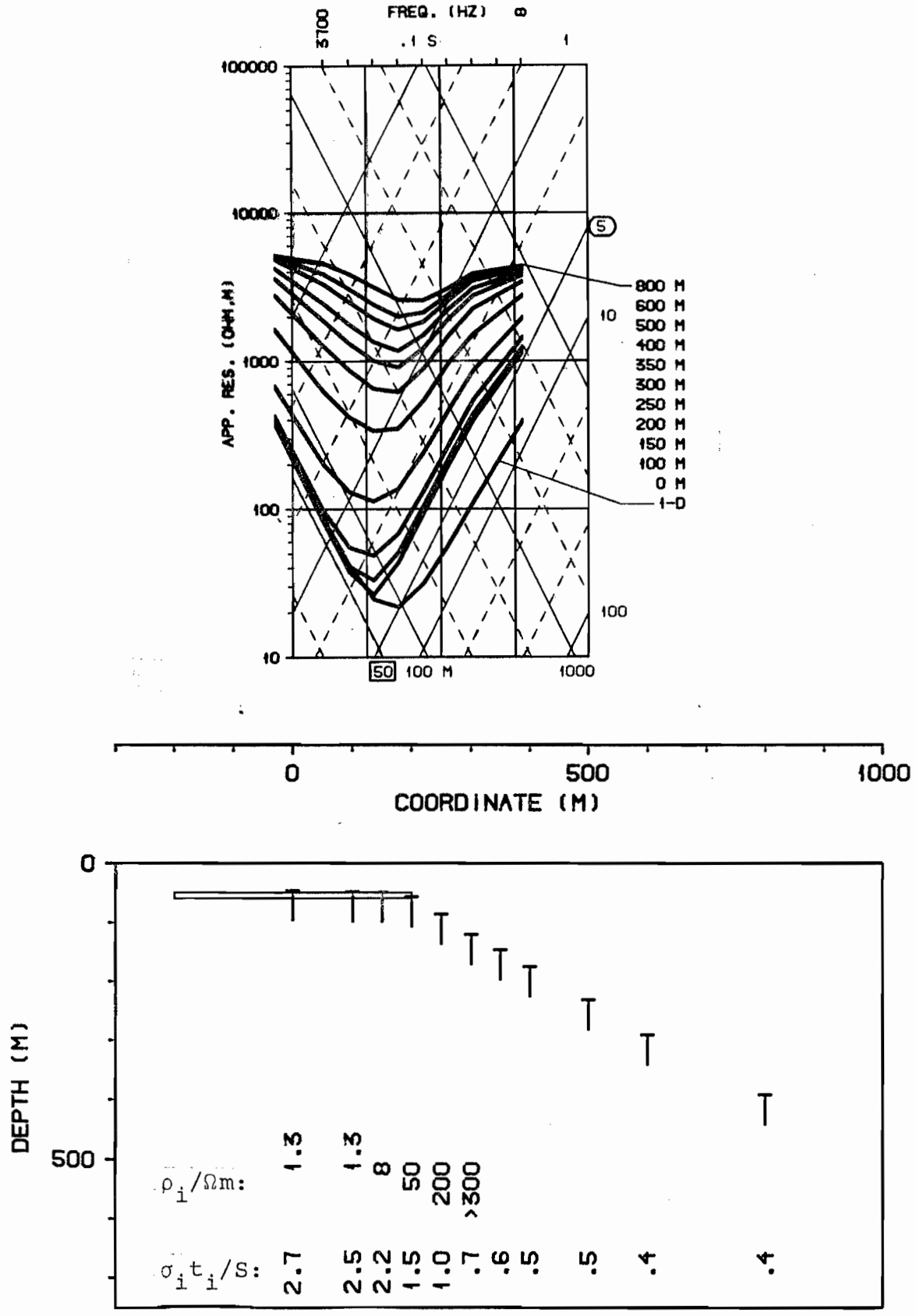

Fig. 11. TE-mode sounding curves over Model 1 with h=50 m and one-dimensional interpretation of them.

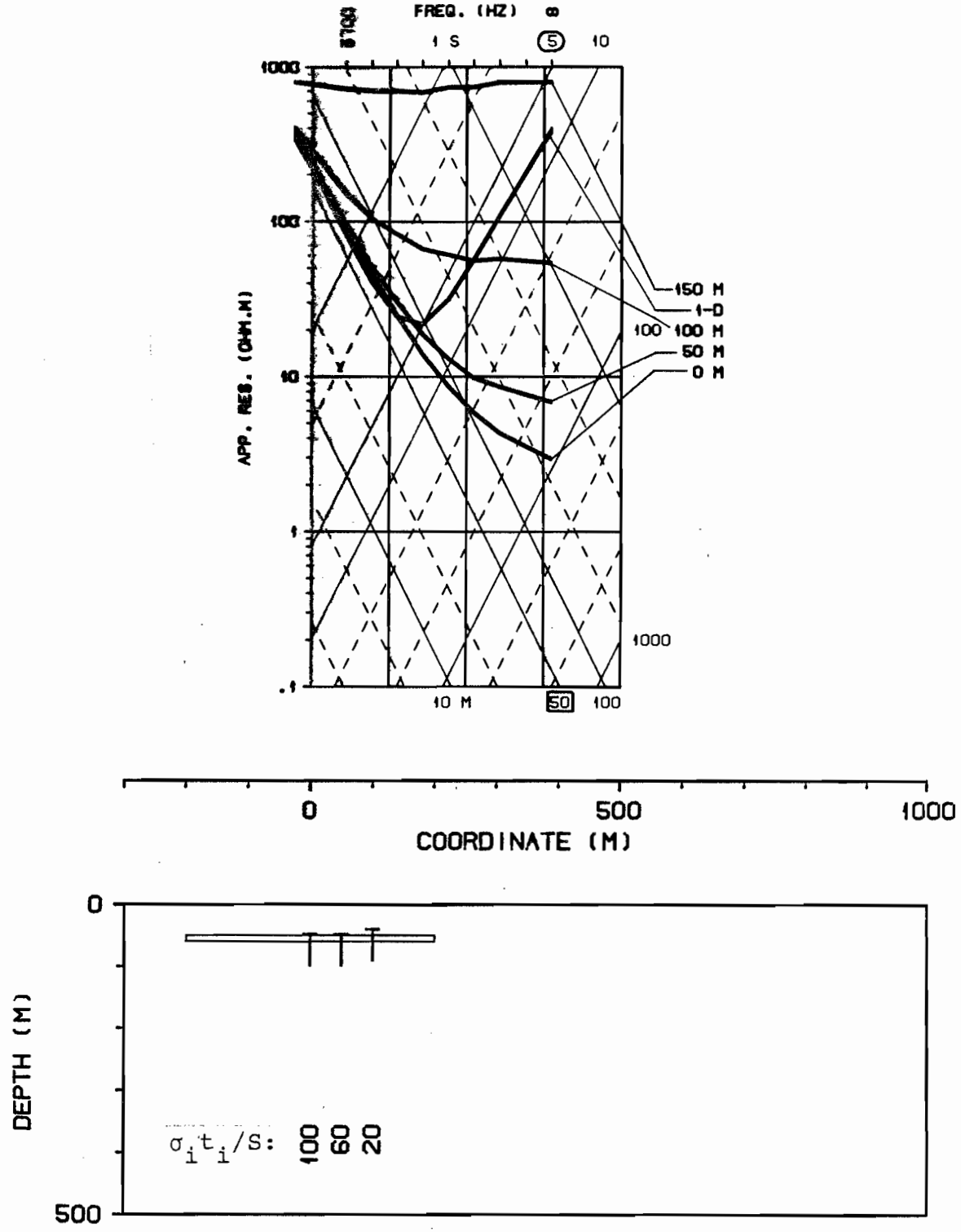

Fig. 12. TM-mode sounding curves over Model 1 with h=50 m and one-dimensional interpretation of them.

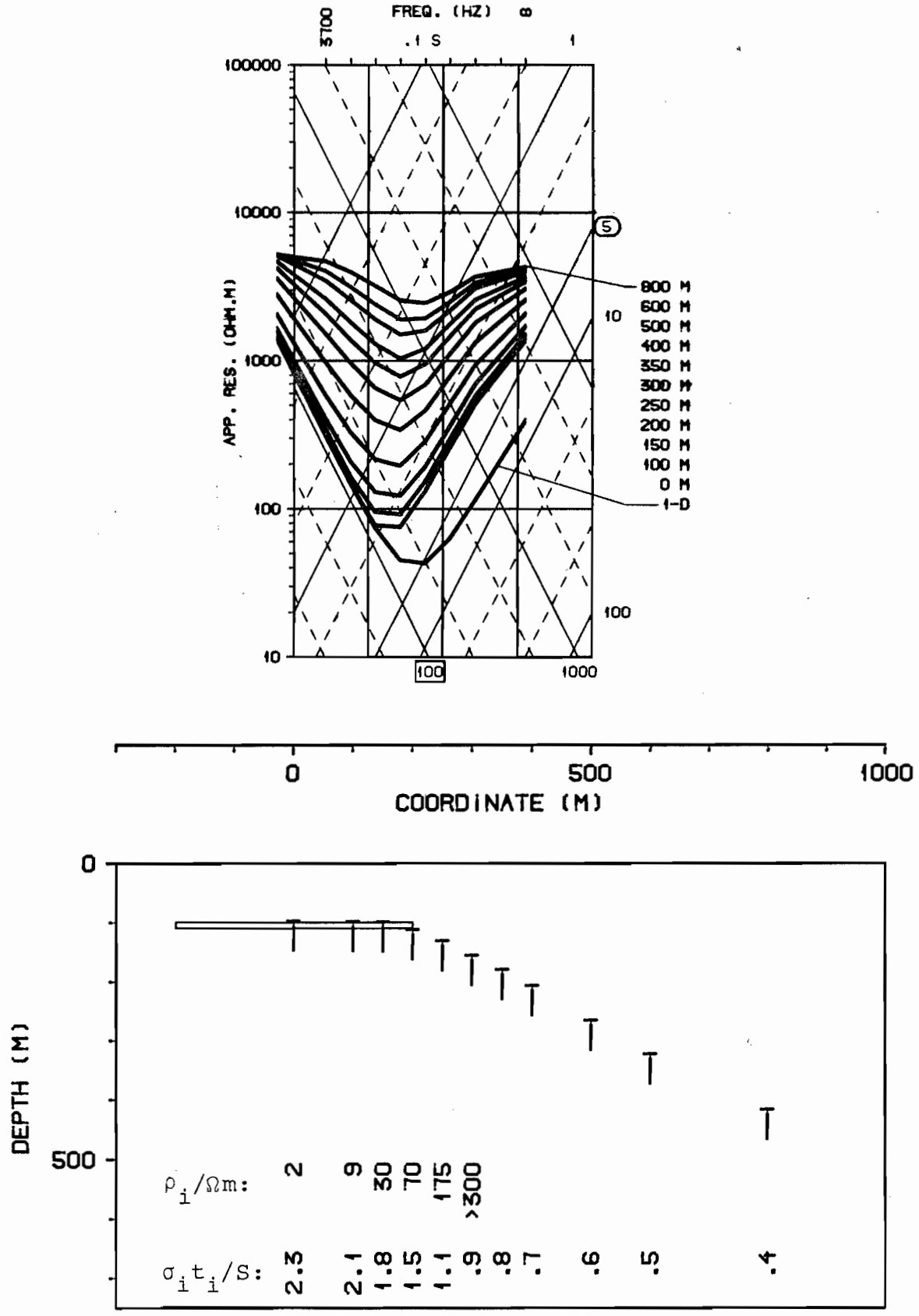

Fig. 13. TE-mode sounding curves over Model 1 with h=100 m and one-dimensional interpretation of them.

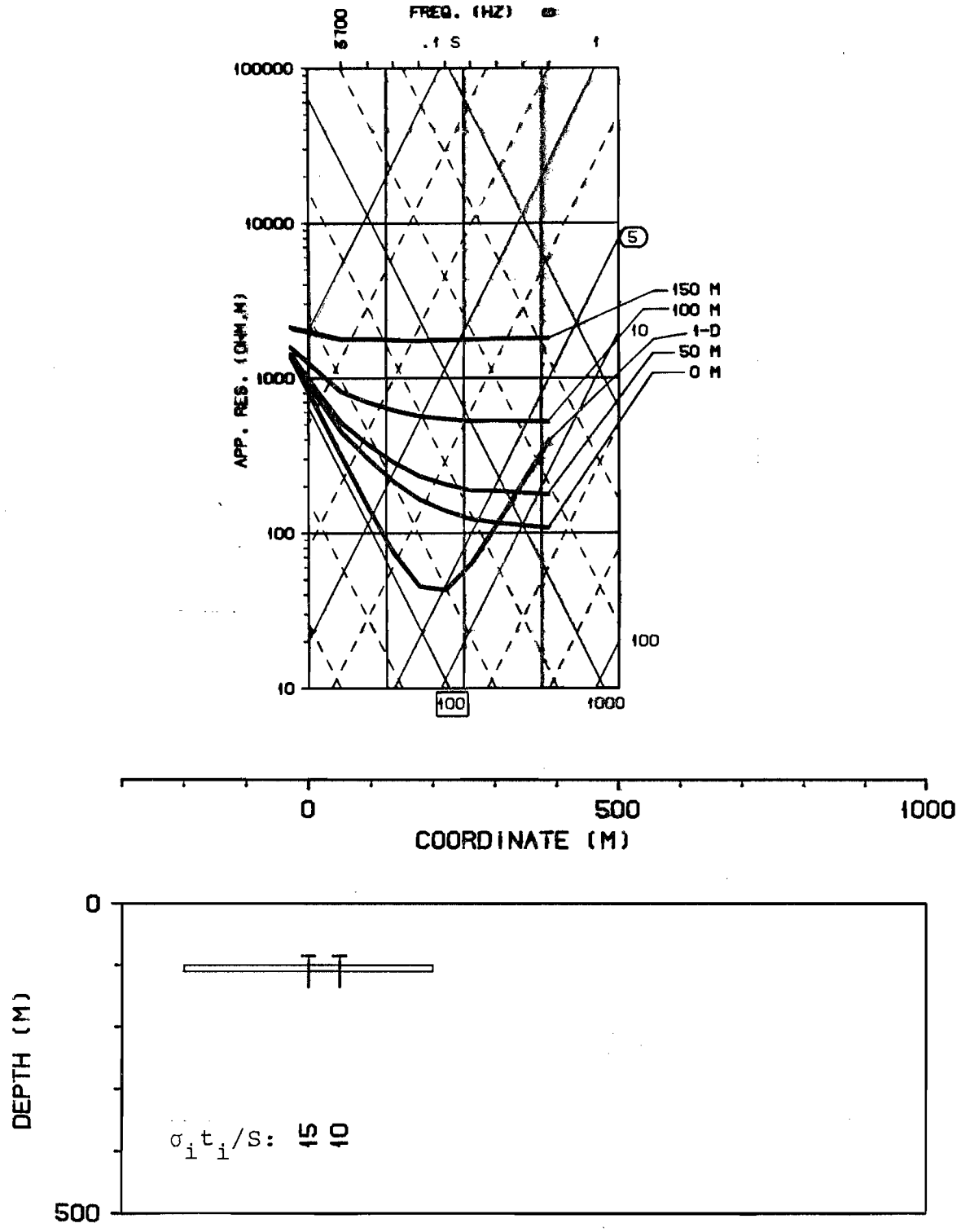

Fig. 14. TM-mode sounding curves over Model 1 with h=100 m and one-dimensional interpretation of them.

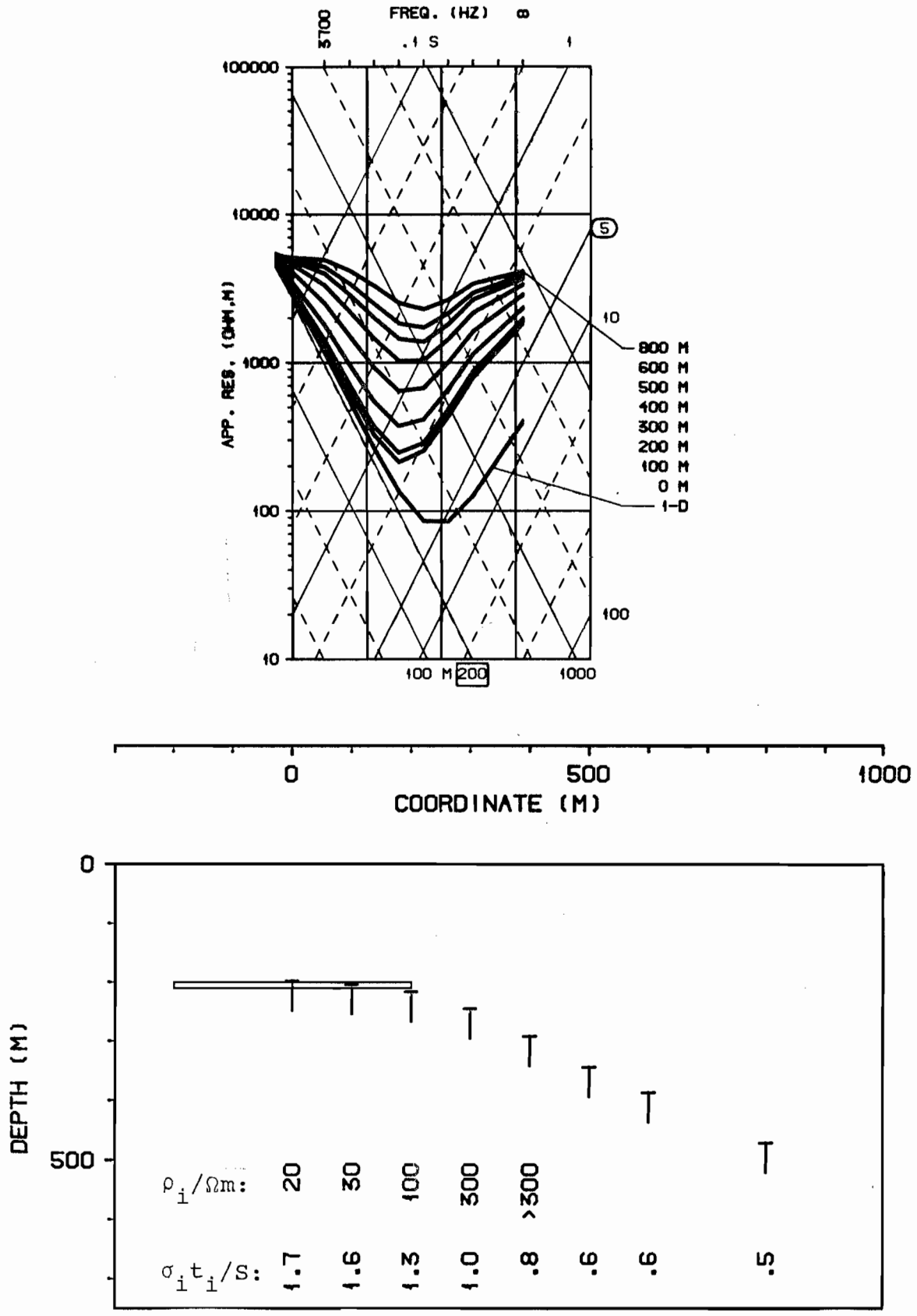

Fig. 15. TE-mode sounding curves over Model 1 with h=200 m and one-dimensional interpretation of them.

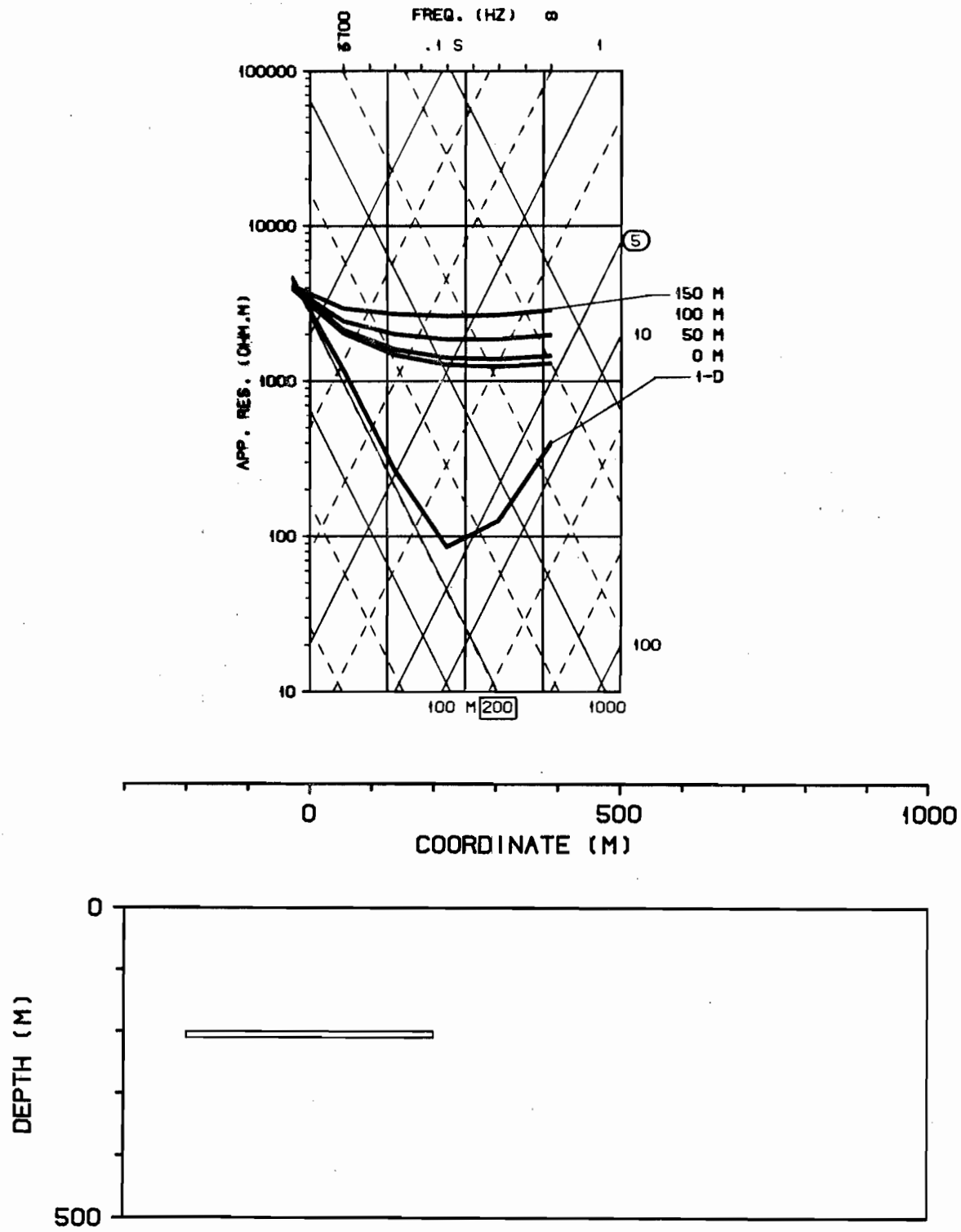

Fig. 16. TM-mode sounding curves over Model 1 with h=200 m. The curves have been calculated only with the frequencies 3700, 800, 170, 37 and 8 Hz and they have not been interpreted.

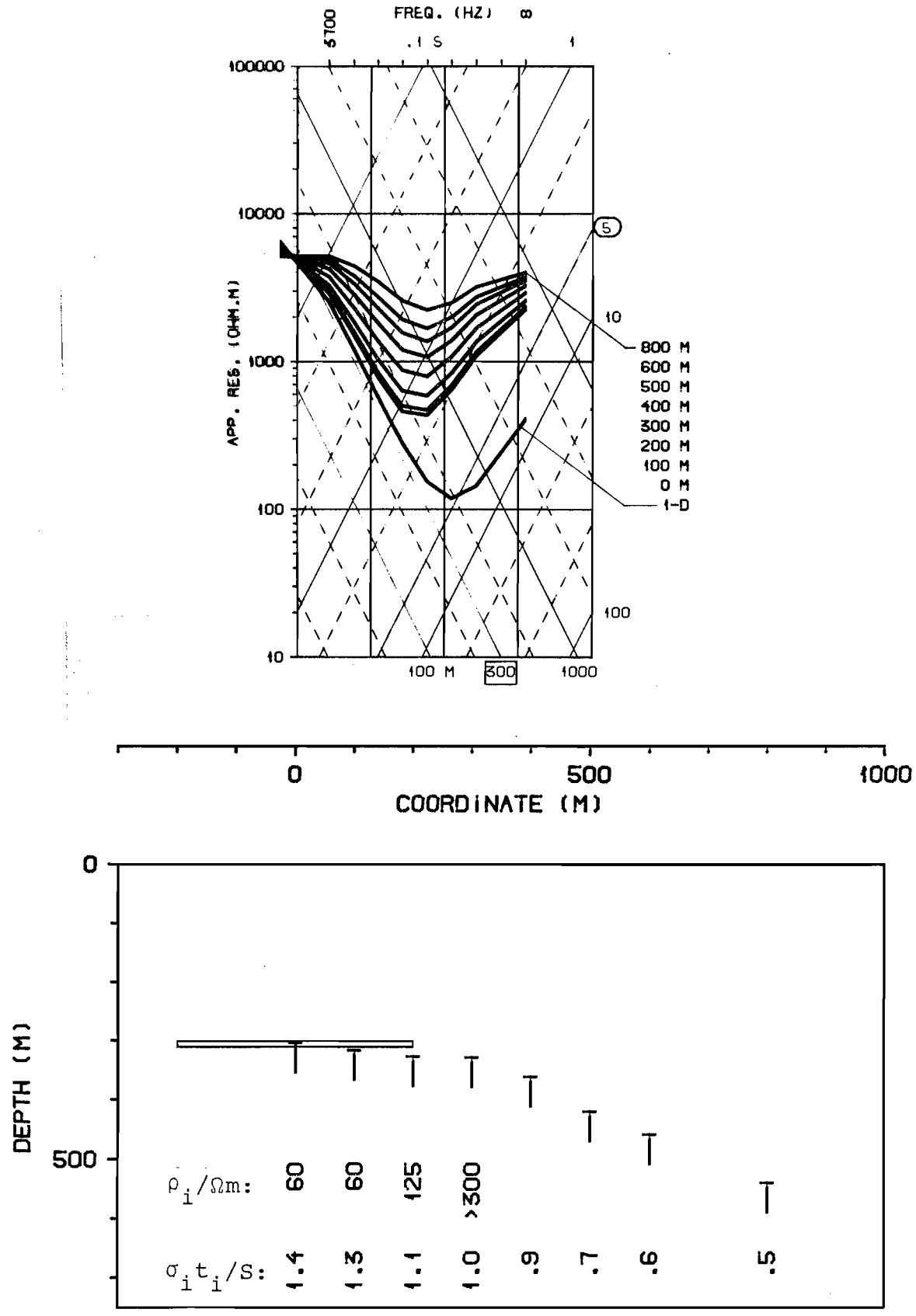

Fig. 17. TE-mode sounding curves over Model 1 with h=300 m and one-dimensional interpretation of them.

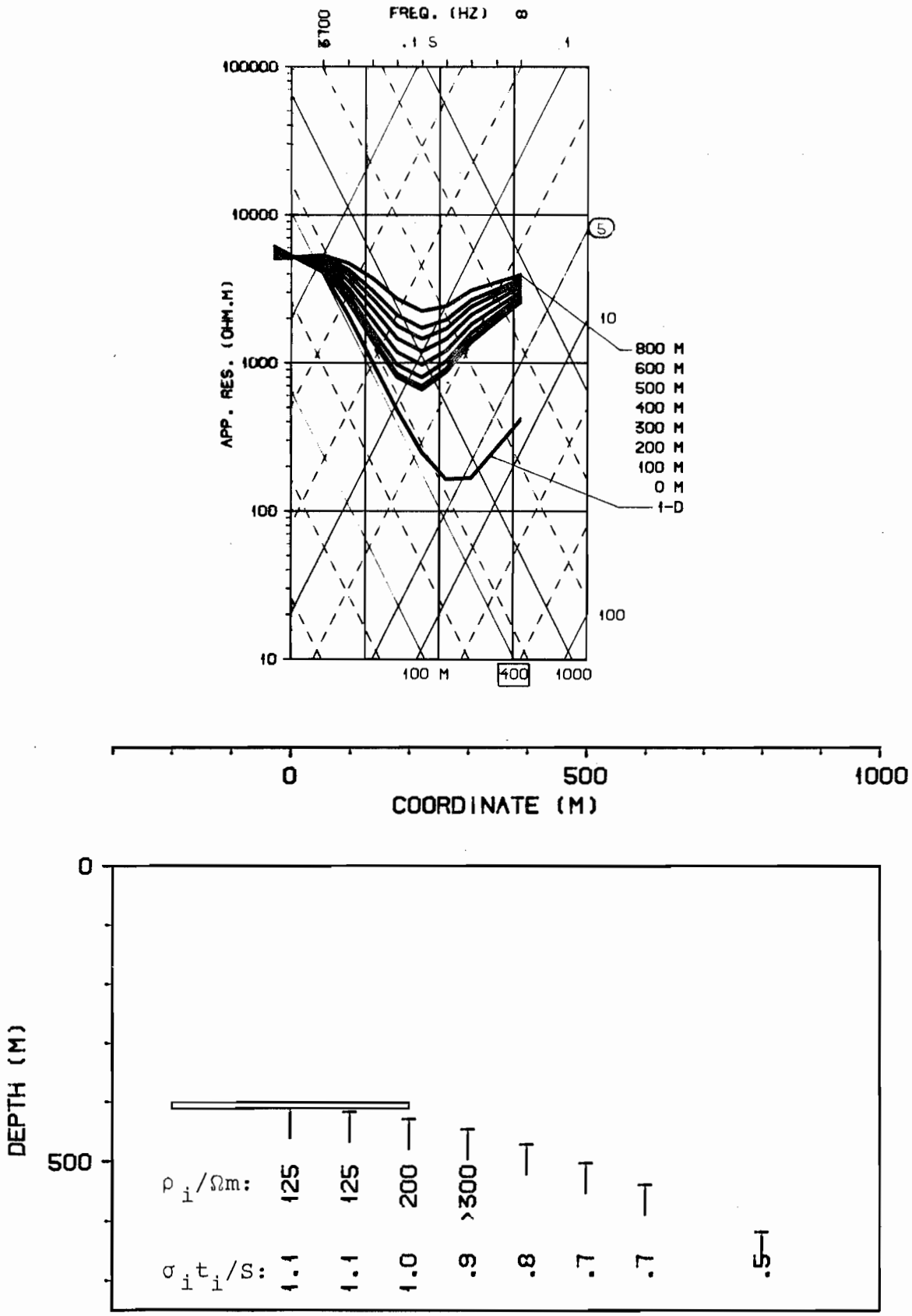

Fig. 18. TE-mode sounding curves over Model 1 with h=400 m and one-dimensional interpretation of them.

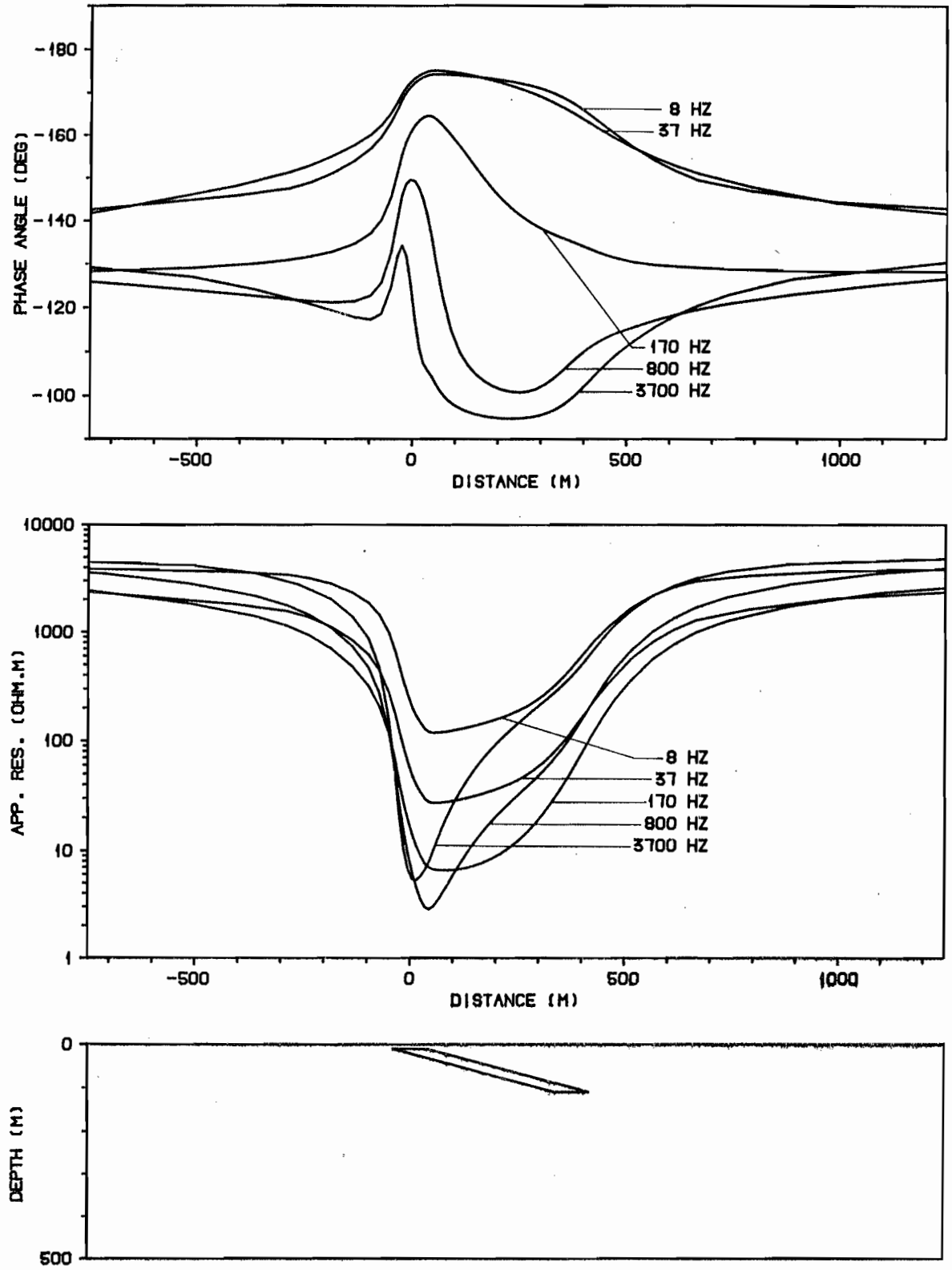

Fig. 19. AMT profiles of TE-mode over Model 2 with Φ=15°.

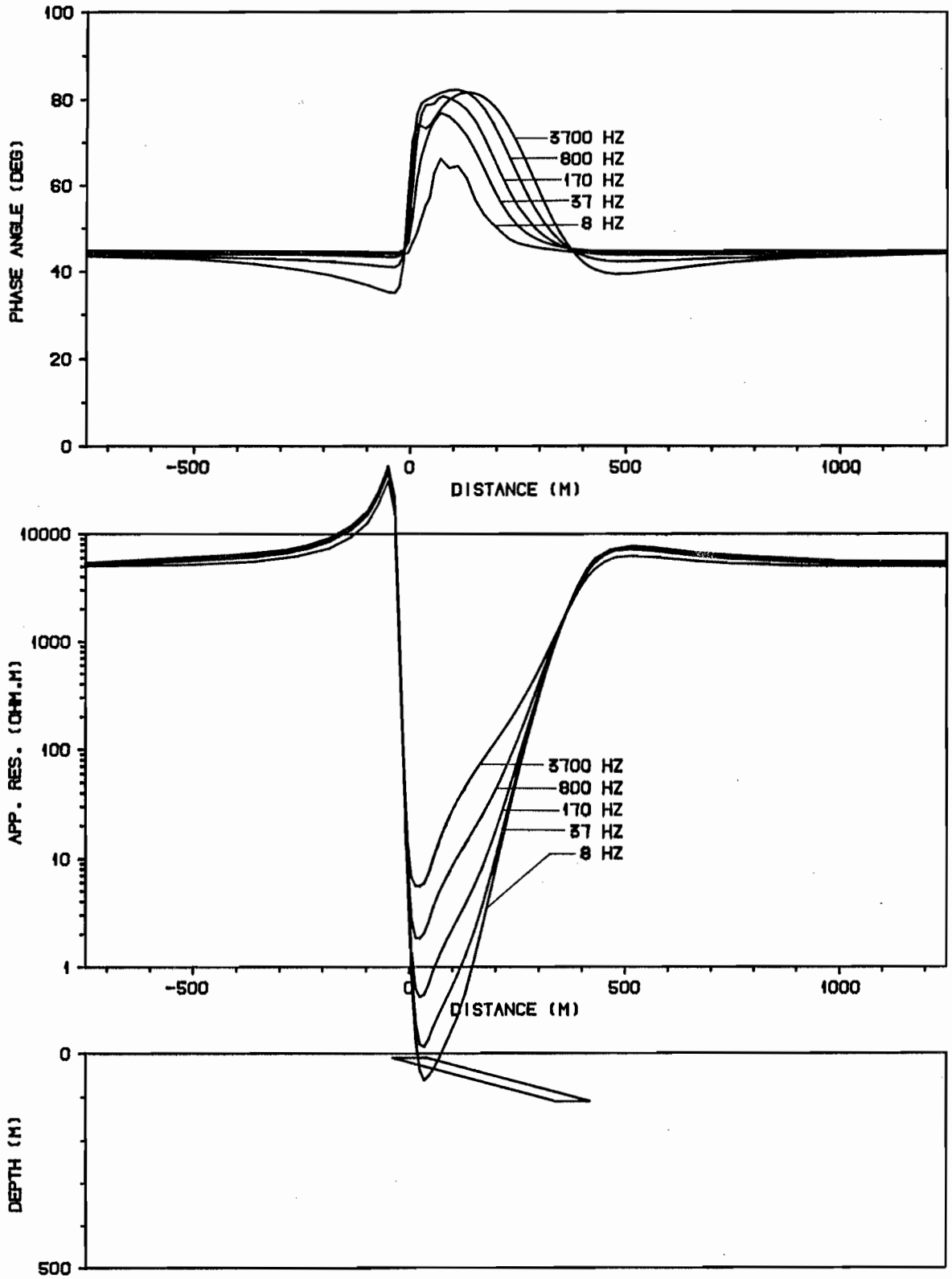

Fig. 20. AMT profiles of TM-mode over Model 2 with $\varphi=15^{o}$. The oscillations in the phase angle profiles of 3700, 170 and 8 Hz are due to poor grids.

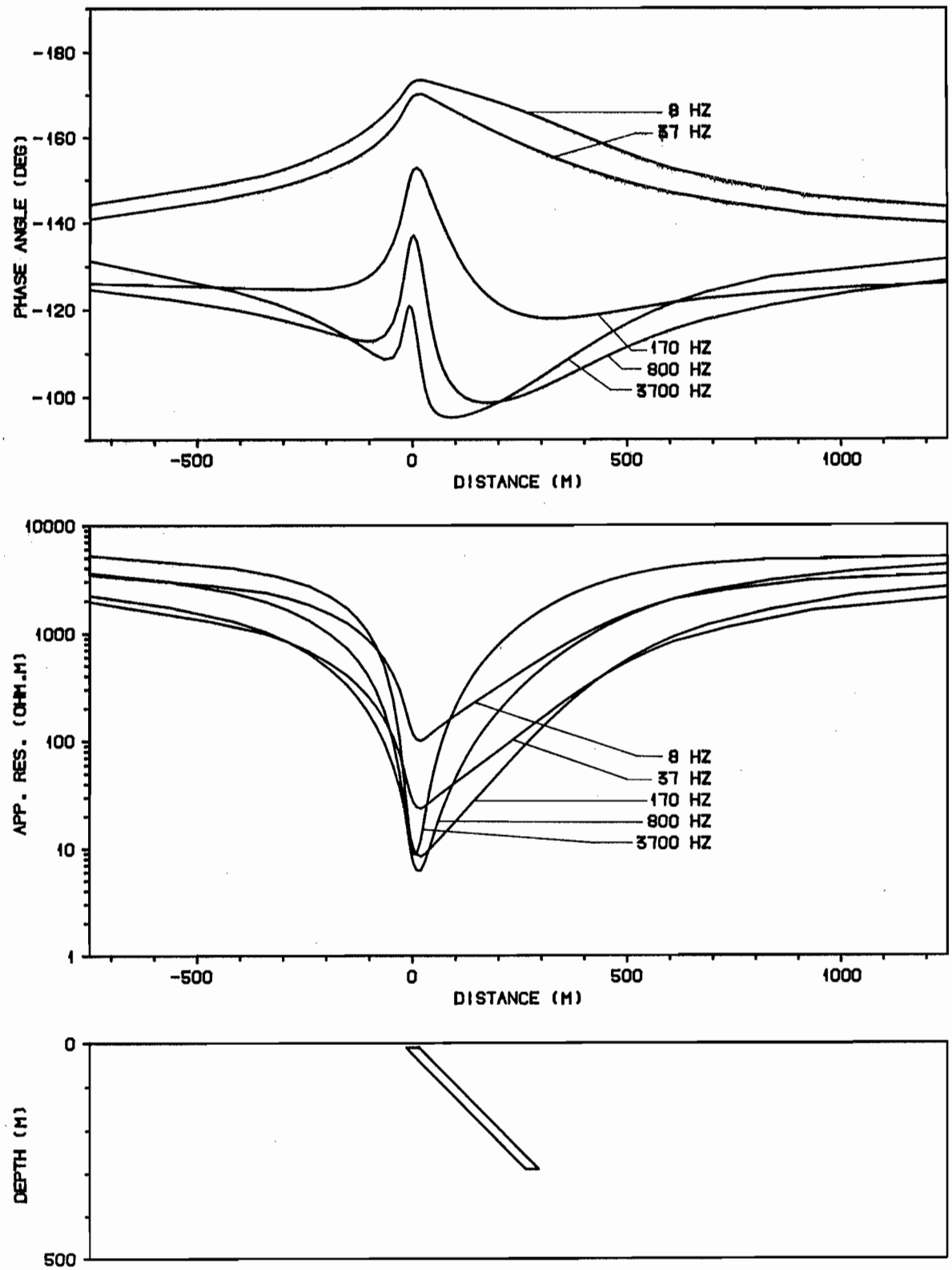

Fig. 21. AMT profiles of TE-mode over Model 2 with $\varphi=45^{o}$.

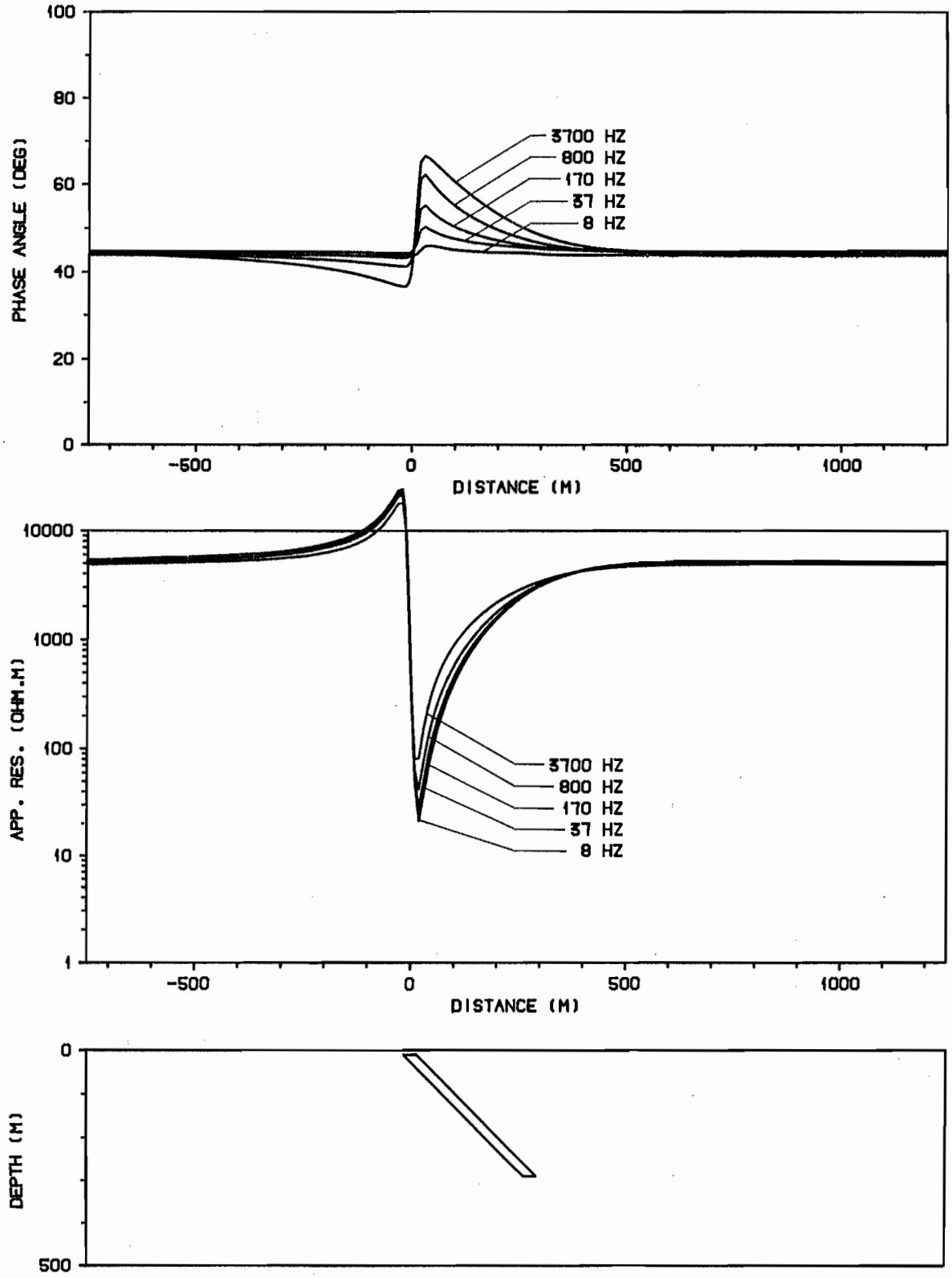

Fig. 22. AMT profiles of TM-mode over Model 2 with $\varphi=45^{o}$.

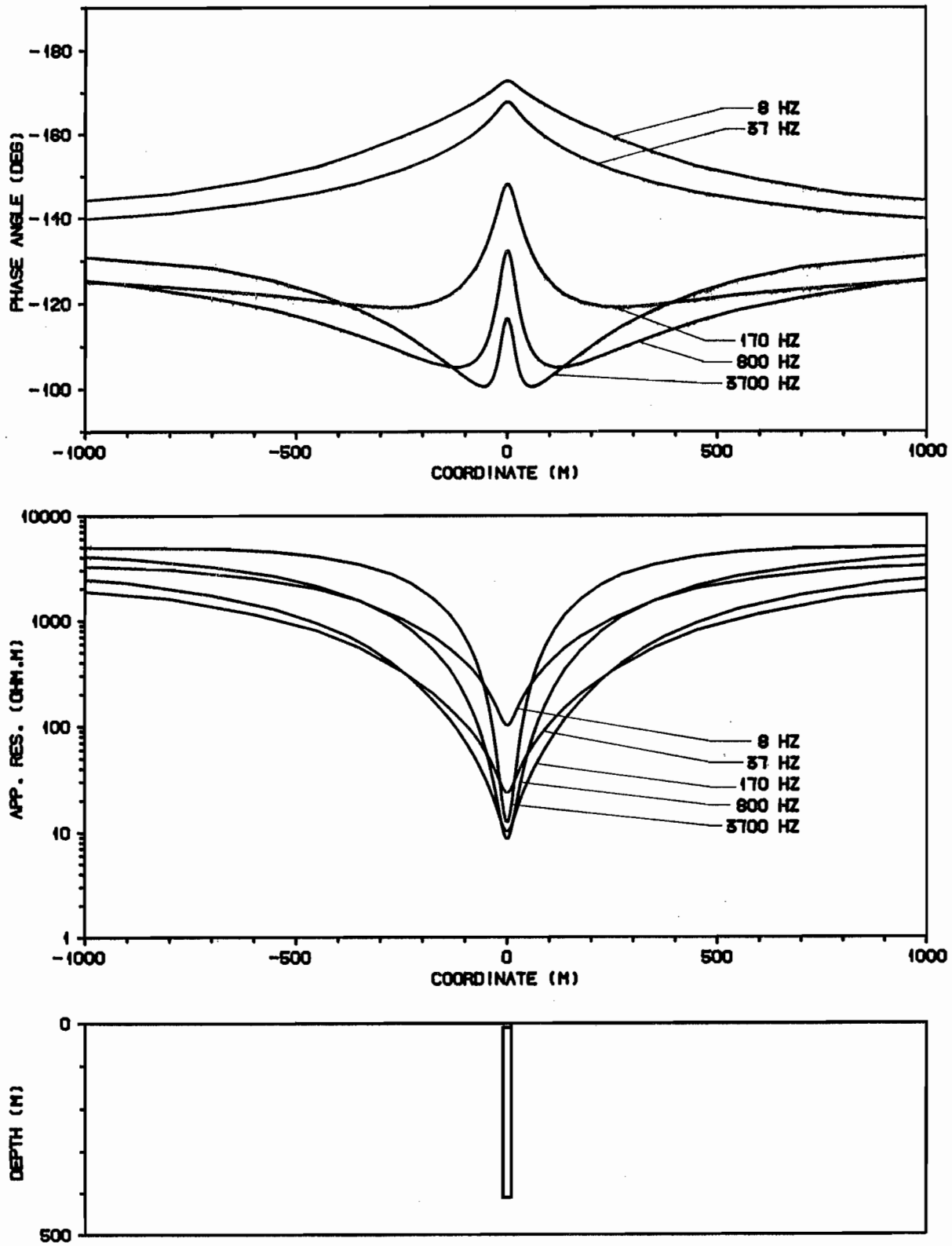

Fig. 23. AMT profiles of TE-mode over Model 2 with $\varphi=90^{o}$.

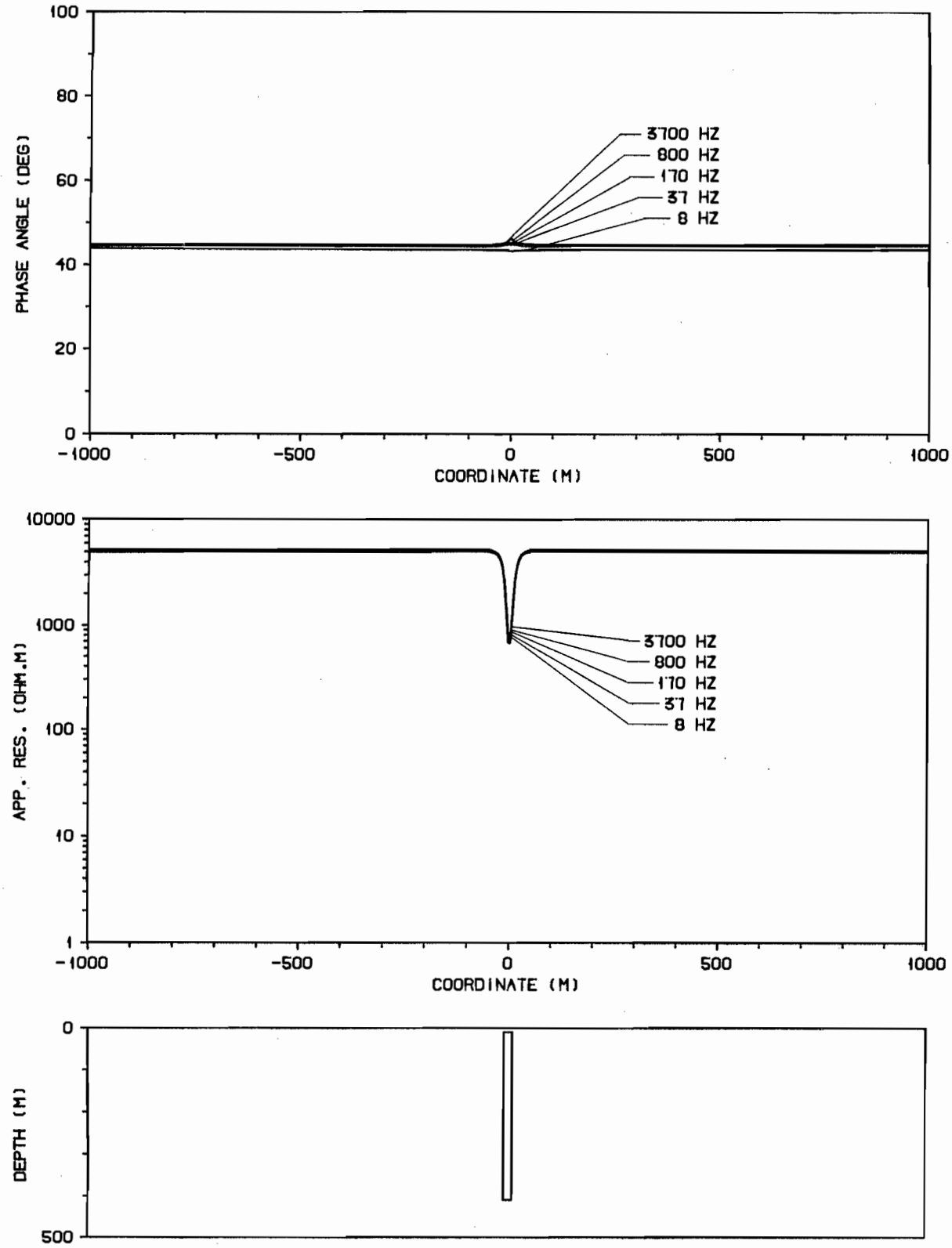

Fig. 24. AMT profiles of TM-mode over Model 2 with $\varphi=90^{o}$.

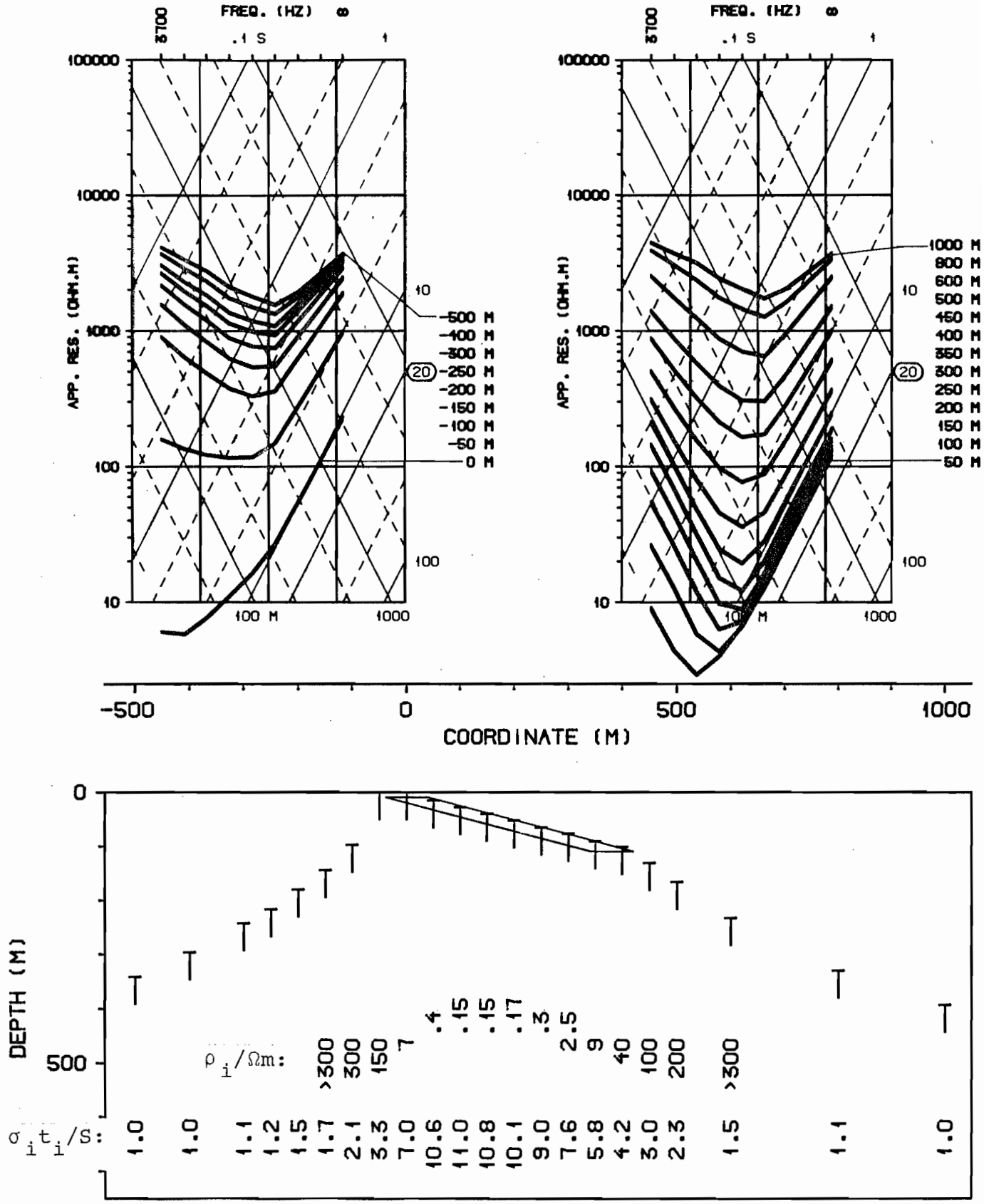

Fig. 25. TE-mode sounding curves over Model 2 with $\varphi=15^{o}$ and one-dimensional interpretation of them.

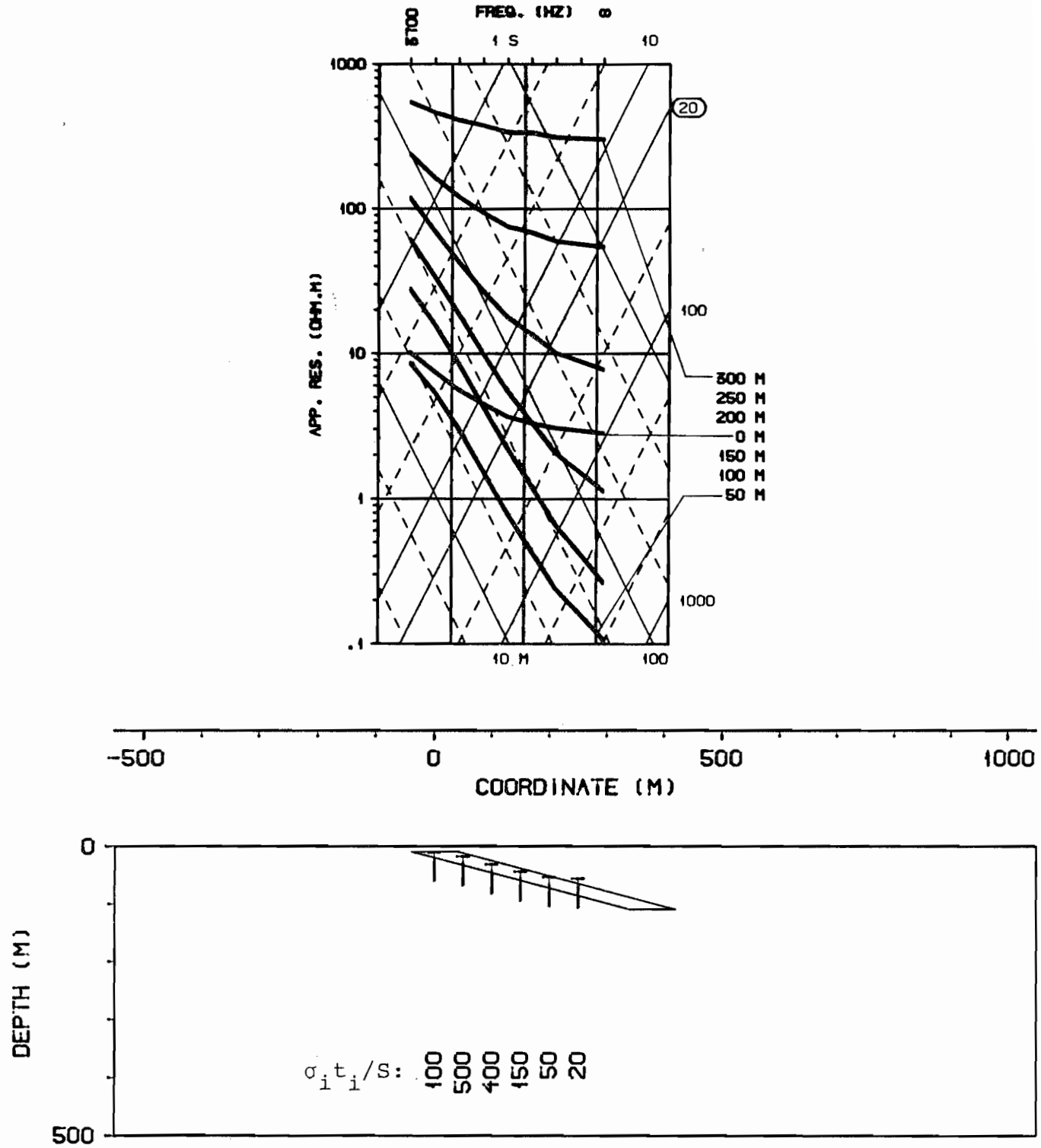

Fig. 26. TM-mode sounding curves over Model 2 with $\varphi = 15^{o}$ and one-dimensional interpretation of them.

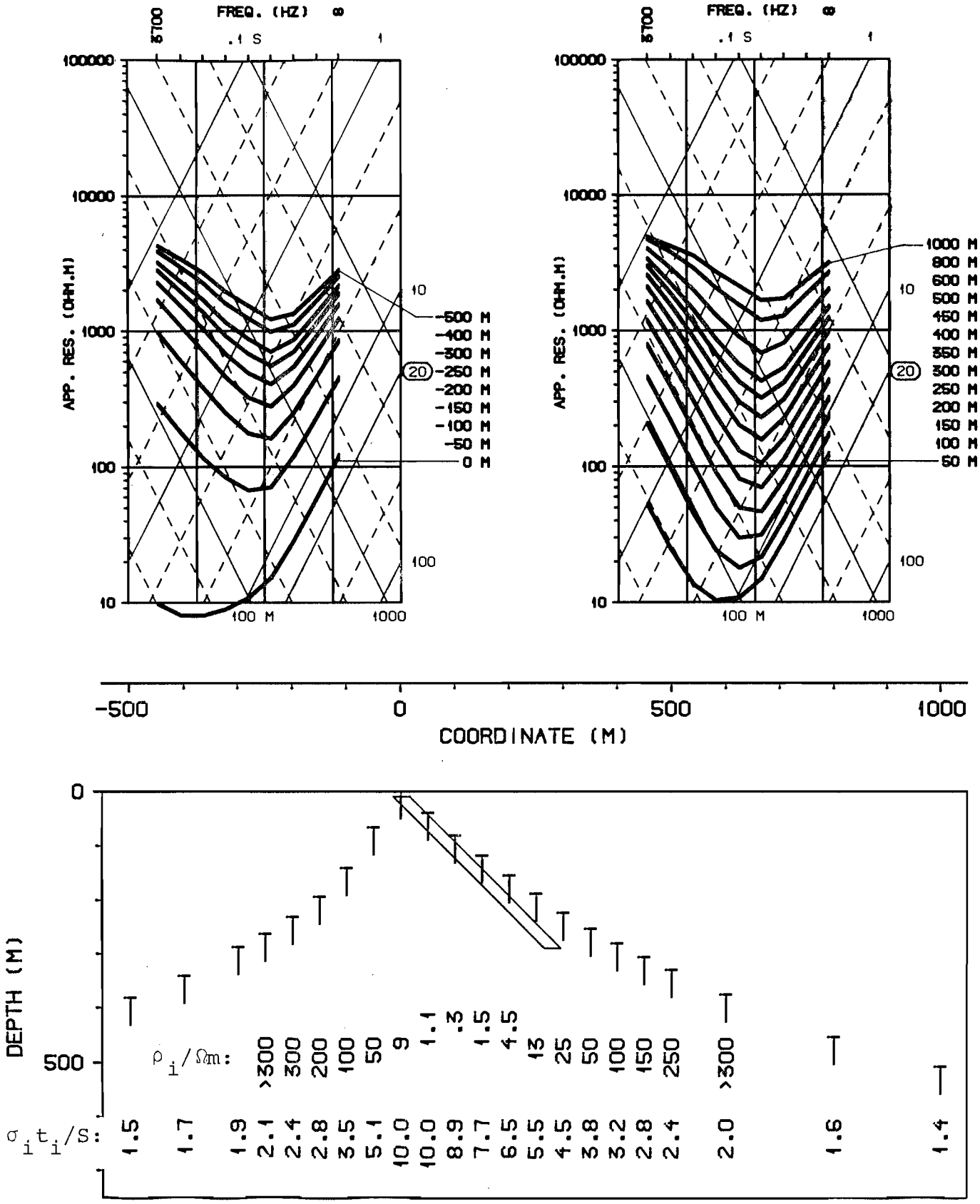

Fig. 27. TE-mode sounding curves over Model 2 with $\varphi=45^{o}$ and one-dimensional interpretation of them.

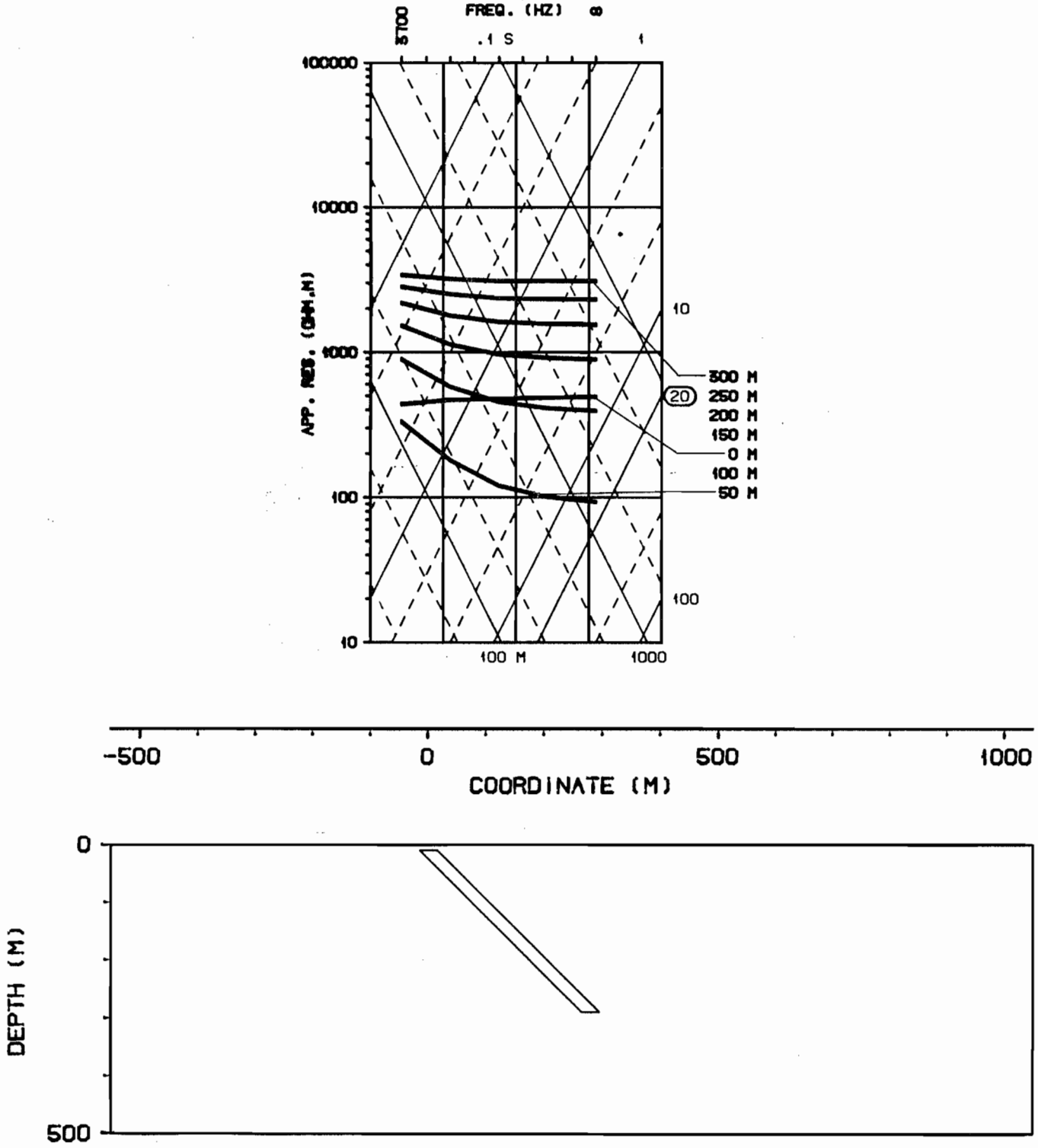

Fig. 28. TM-mode sounding curves over Model 2 with $\varphi=45^{o}$. The curves have been calculated only with the frequencies 3700, 800, 170, 37 and 8 Hz and they have not been interpreted.

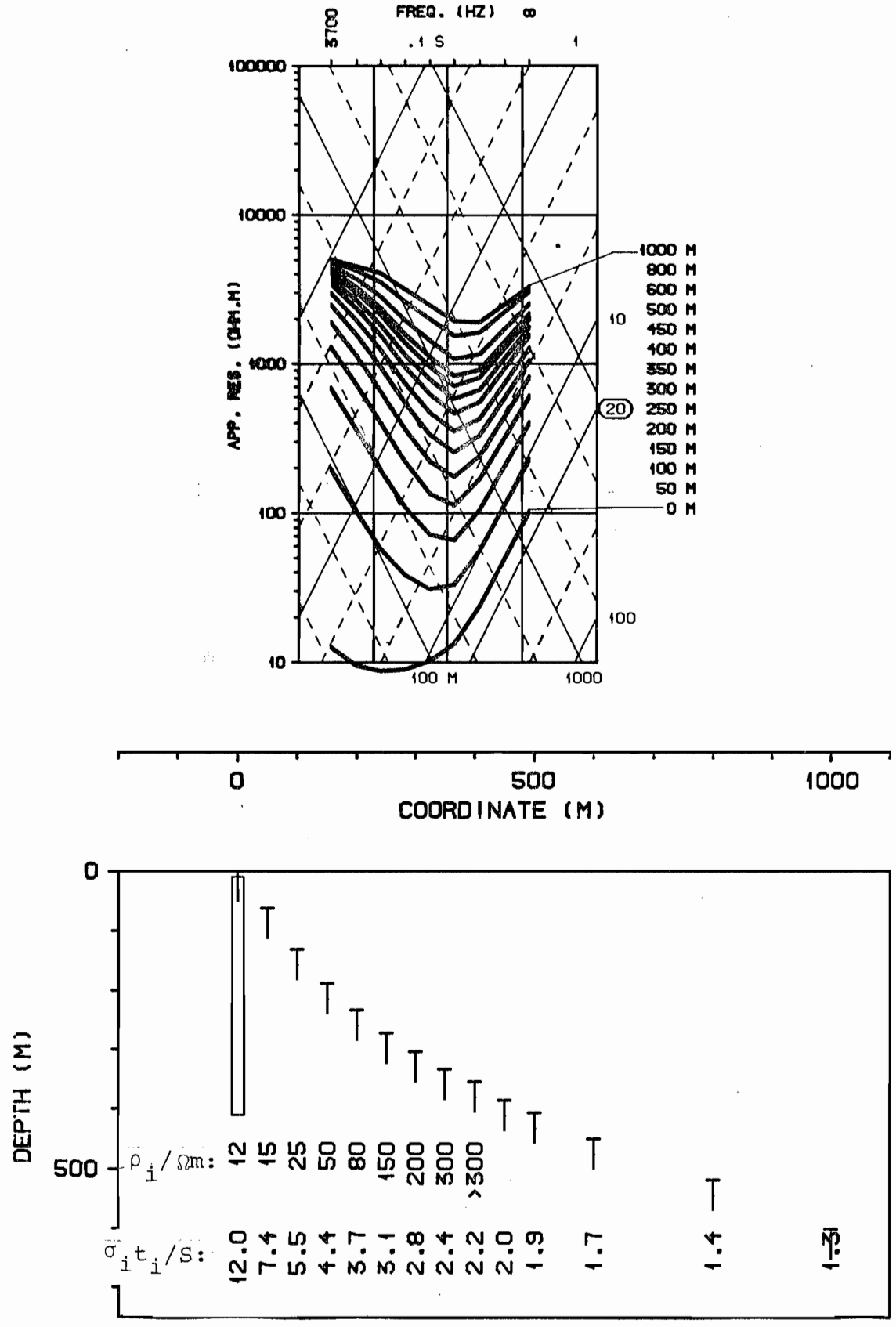

Fig. 29. TE-mode sounding curves over Model 2 with $\varphi=90^{\circ}$ and one-dimensional interpretation of them.

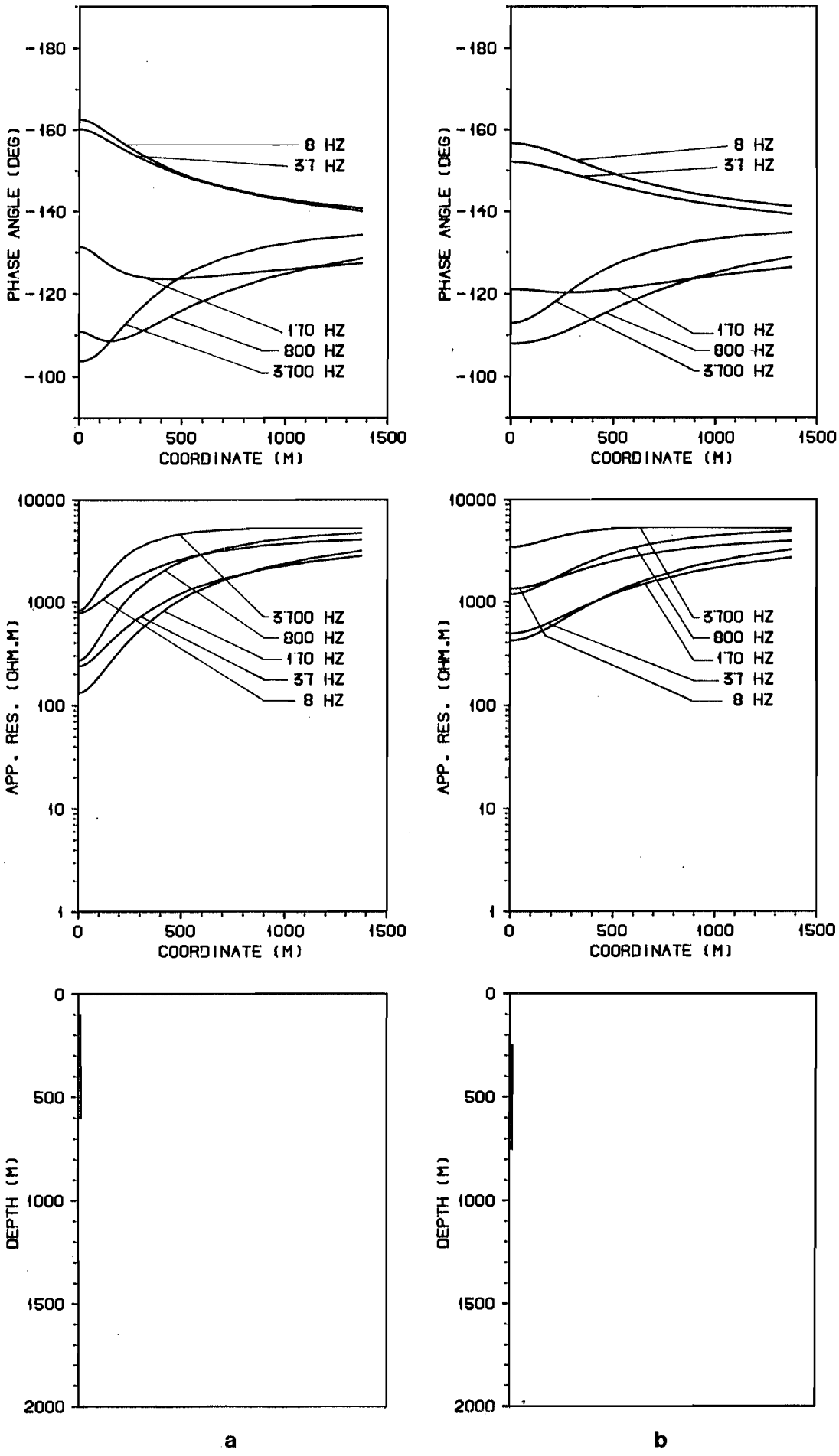

Fig. 30. AMT profiles of TE-mode over Model 3 with h=100 m (a) and h=250 m (b).

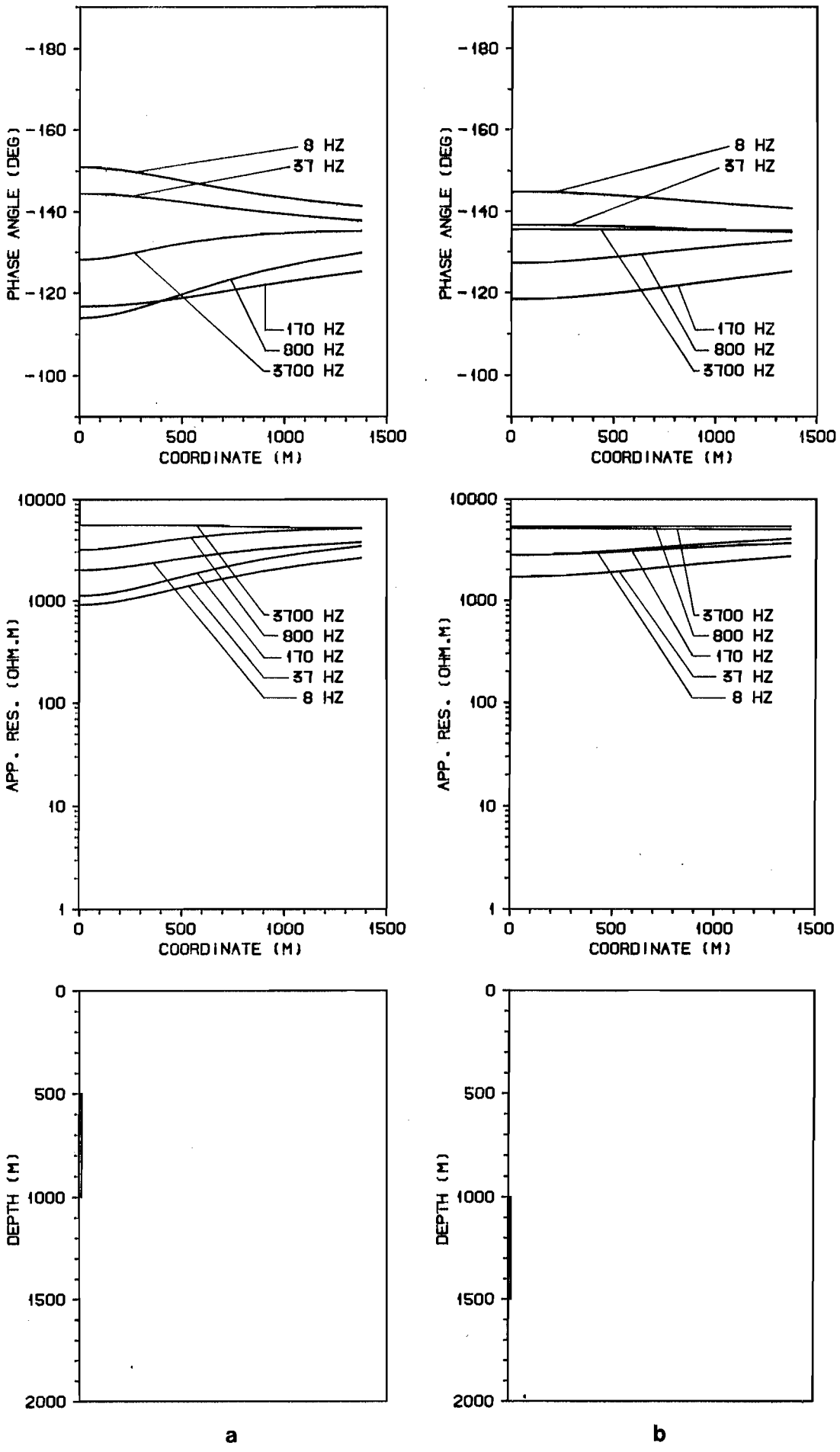

Fig. 31. AMT profiles of TE-mode over Model 3 with h=500 m (a) and h=1000 m (b).

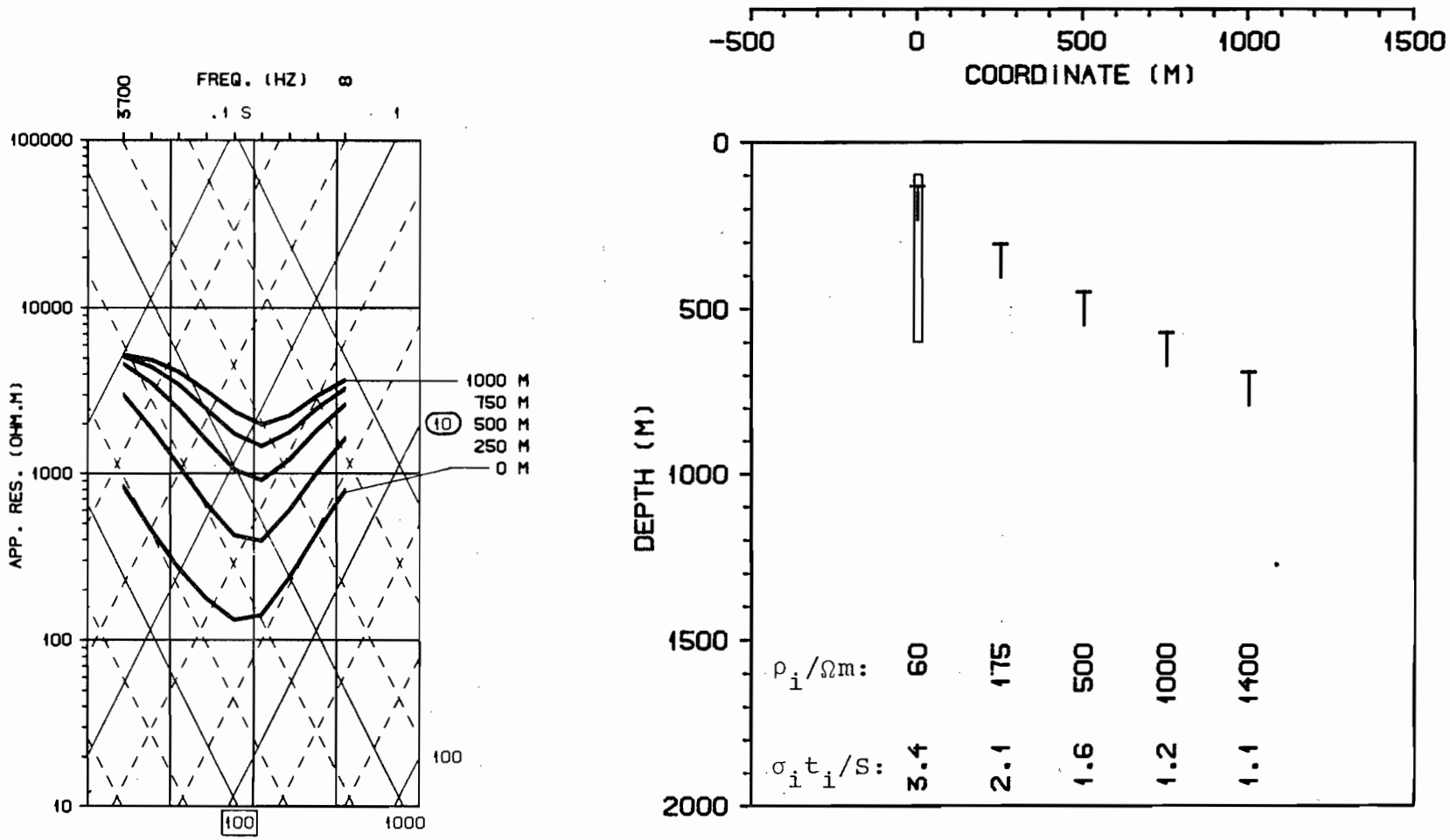

Fig. 32. TE-mode sounding curves over Model 3 with h=100 m and one-dimensional interpretation of them.

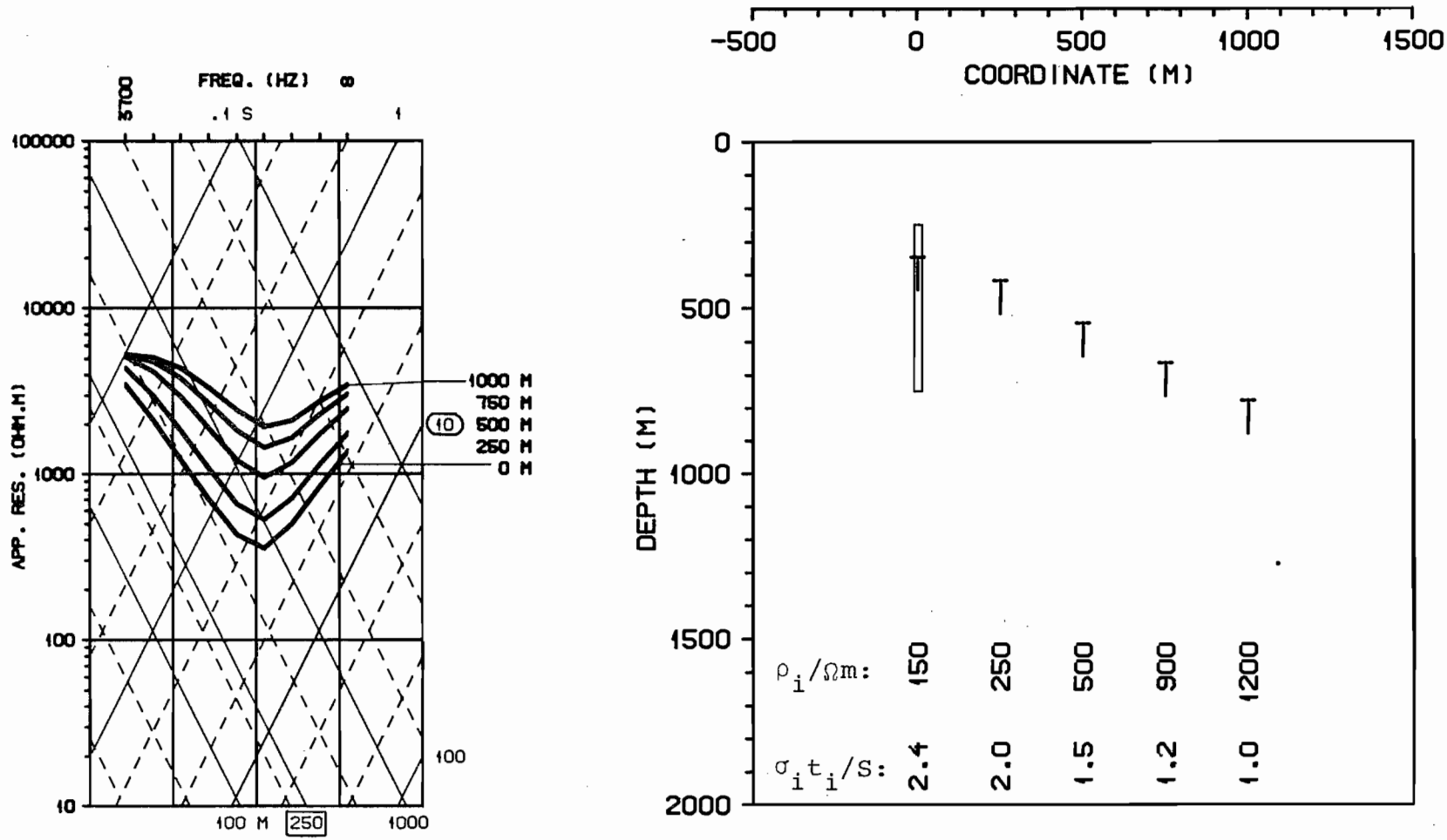

Fig. 33. TE-mode sounding curves over Model 3 with h=250 m and one-dimensional interpretation of them.

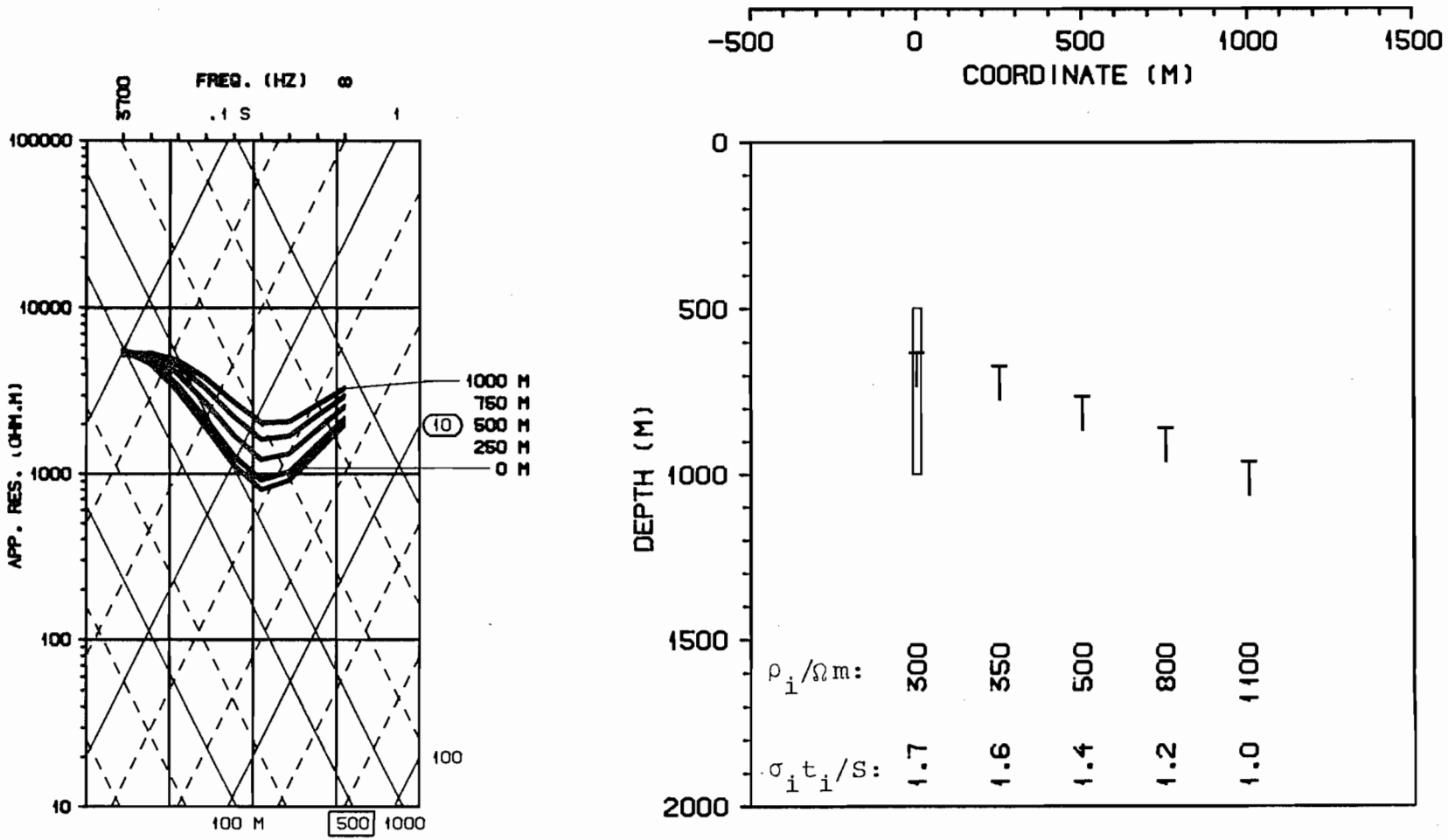

Fig. 34. TE-mode sounding curves over Model 3 with h=500 m and one-dimensional interpretation of them.

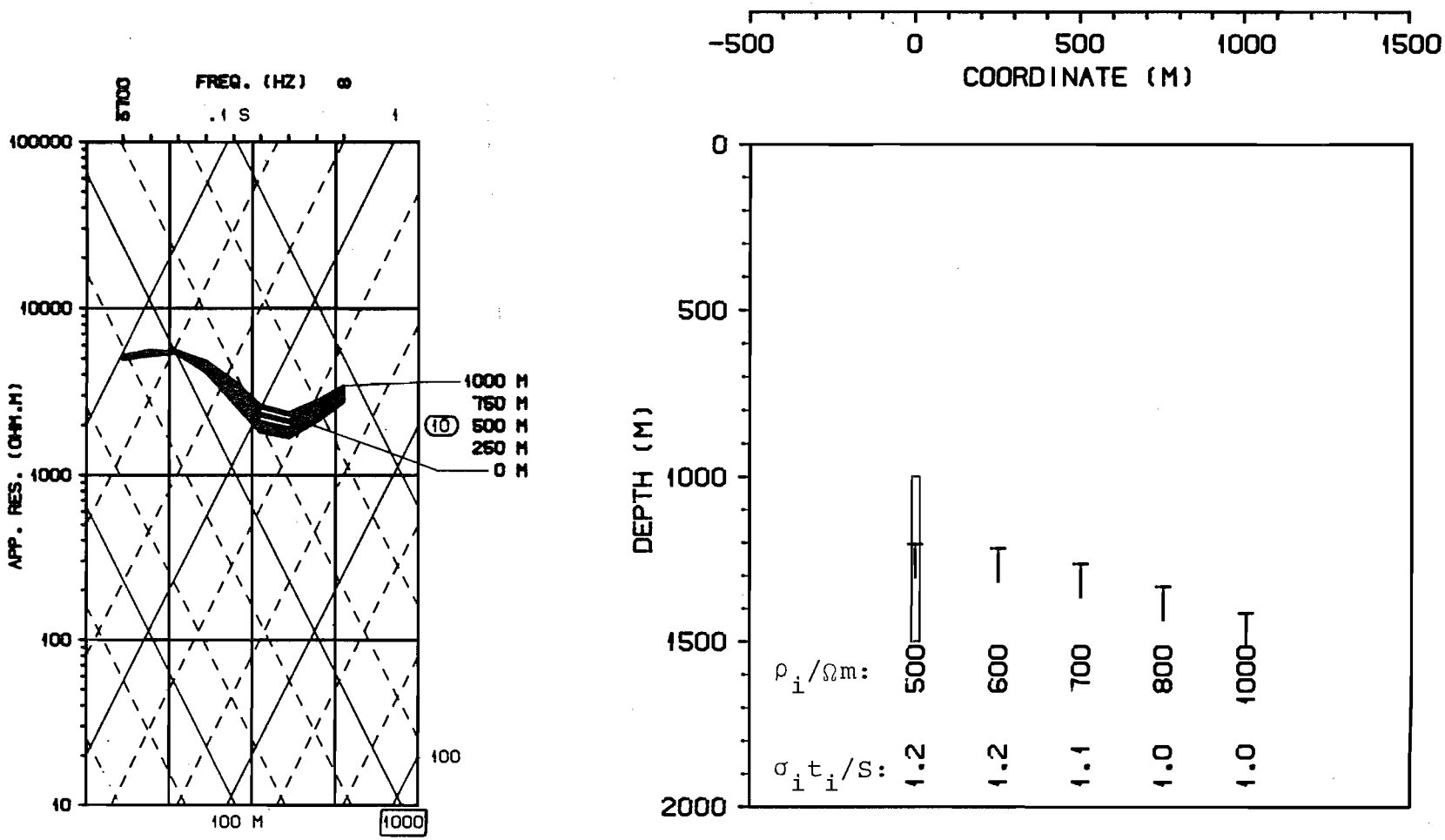

Fig. 35. TE-mode sounding curves over Model 3 with h=1000 m and one-dimensional interpretation of them.

Reports

1. S.E. Hjelt, A.Ph. Phokin (editors), 1981: Interpretation of borehole magnetic data and some special problems of magnetometry. Department of Geophysics, University of Oulu, Report No. 1.
2. M. Karous and T. Pernu, 1982: Asymmetrical resistivity sounding-profiling with three-electrode gradient arrays AMN- MNB. Department of Geophysics, University of Oulu, Report No. 2.
3. M. Karous, 1982: Gradient curves in resistivity measurements with some asymmetric electrode configurations. Department of Geophysics, University of Oulu, Report No. 3.
4. H. Arkimaa and J. Raitala, 1982: The mapping of small lakes using Landsat data: a pilot study. Department of Geophysics, University of Oulu, Report No. 4.
5. S.E. Hjelt (ed.), 1982: Geophysical and geodetic research in Finland and Hungary. Papers presented at the Symposium of the Section Geodesy-Geophysics, Oulu, September 1st 1981 during the Days of Hungarian Science 1981. Department of Geophysics, University of Oulu, Report No. 5.
6. E. Lanne, 1982: Comparison of some isotropic rock models with a high electrical resistivity contrast between mixture phases. Department of Geophysics, University of Oulu, Report No. 6.
7. S.E. Hjelt and L.L. Vanyan (editors), 1983: The development of the deep geoelectric model of the Baltic Shield. Part 1. Numerical methods. Department of Geophysics, University of Oulu, Report No. 7.
8. S.E. Hjelt (ed.), 1984: The development of the deep geoelectric model of the Baltic Shield. Part 2. Proceedings of the 1st project symposium, Oulu 15.-18.11.1983. Department of Geophysics, University of Oulu, Report No. 8.
9. E. Lanne, 1984: Some basic features of the statistical interpretation of airborne gamma-ray observations. Department of Geophysics, University of Oulu, Report No. 9.
10. K. Pajunpää, 1984: Recordings of the geomagnetic variations with two-dimensional magnetometer arrays in Finland 1981-1983. Department of Geophysics, University of Oulu, Report No. 10.